

**FABRICATION AND KINETIC MODELING OF CYTOCHROME P450_{2D6}
AMPEROMETRIC BIOSENSORS FOR SEROTONIN REUPTAKE
INHIBITORS**

NTLATSENG GRETТА RHODA MATHEBE



A full thesis submitted in partial fulfilment of the requirements for the degree of
Magister Scientiae in the Department of Chemistry, University of the Western
Cape.

Supervisor: Prof. Emmanuel I Iwuoha

December 2005

KEYWORDS

Amperometric Biosensor

Polyaniline

Cytochrome P450_{2D6}

Serotonin Reuptake Inhibitors

Fluoxetine

Fluvoxamine

Quinidine

N-Demethylation

Cyclic Voltammetry

Screen-Printed Electrode



ABSTRACT

An amperometric biosensor was prepared by *in situ* deposition of cytochrome P450_{2D6} (CYP2D6, P450_{2D6}) enzyme on a polyaniline (PANI)-doped glassy carbon electrode. The PANI film was electrochemically deposited on the electrode at 100 mV s⁻¹ against Ag/AgCl. Cyclic voltammetric characterisation of the PANI film in 1 M HCl solution showed two distinct redox peaks, which prove that the PANI film was electroactive and exhibited fast reversible electrochemistry. The surface concentration and film thickness of the adsorbed electroactive species was estimated to be 1.85×10^{-7} mol cm⁻² and approximately 16 nm, respectively.

Cytochrome P450_{2D6} was electrostatically immobilised onto the surface of the PANI film and cyclic voltammetry was used to monitor the serotonin reuptake inhibitors (fluoxetine, fluvoxamine and citalopram) in phosphate buffer solution. Fluoxetine was found to be a substrate of CYP2D6 at low concentrations but inhibits enzyme activity at high concentrations; this was consistent with uncompetitive substrate inhibition kinetics. Thus PANI-mediated electrochemistry can be used to observe monooxygenation reaction of CYP2D6.

DECLARATION

I declare that *Fabrication and Kinetic Modeling of Cytochrome P450_{2D6} Amperometric Biosensors for Serotonin Reuptake Inhibitors* is my own work, that it has not been submitted before for any degree or examination in any other university, and that all the sources I have used or quoted have been indicated and acknowledged as complete references.



Ntlatseng Gretta Rhoda Mathebe

December 2005

Signed:

ACKNOWLEDGEMENTS

Firstly I would like to give thanks to God the Almighty for seeing me through this journey.

To my supervisor, Prof. Emmanuel Iwuoha, my sincere thanks for giving me the opportunity to be your student, for your guidance, direction and support throughout my studies.

The Department of Chemistry and its technical staff, and the technical staff in the Department of Physics thank you for all your help.

To my sponsor, NRF, thank you for the funding of my studies and attendance of conferences.

To my family, especially my mother thanks for the motivation and the support throughout my studies.



To all my friends who helped me make this a success, through your understanding, encouragement and support, thank you.

Lastly, to my kids, Onkabetse, Omolemo and Odirile, this is for you. Thank you very much for understanding and putting up with me during my studies, you are the best!

LIST OF PUBLICATIONS

1. **N. G. R. Mathebe**, A. Morrin, E. I. Iwuoha, 2004. Electrochemistry and scanning electron microscopy of polyaniline/peroxidase-based biosensor. *Talanta*, 64: 115-120.
2. E. I. Iwuoha, A. R. Williams-Dottin, L. A. Hall, A. Morrin, **G. N. Mathebe**, M. R. Smyth, A. Killard, 2004. Electrochemistry and application of a novel monosubstituted squarate electron-transfer mediator in a glucose oxidase-doped poly(phenol) sensor. *Pure and Applied Chemistry*, 76: 789-799.
3. E. I. Iwuoha, A. Wilson, M. Howel, **N. G. R. Mathebe**, K. Montane-Jaime, D. Narinesingh, A. Guiseppi-Ellie, 2004. Cytochrome P450_{2D6} (CYP2D6) bioelectrode for fluoxetine. *Analytical Letters*, 37: 929-941.

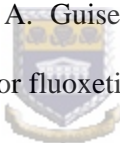



TABLE OF CONTENTS

<i>Title page</i>	i
<i>Keywords</i>	ii
<i>Abstract</i>	iii
<i>Declaration</i>	iv
<i>Acknowledgements</i>	v
<i>List of Publications</i>	vi
<i>List of Figures</i>	x
<i>List of Tables</i>	xii

Chapter 1	Literature Review	1
		
	Introduction	2
1.1.	Biosensors	3
1.1.1.	Biological component	3
1.1.2.	Transducers	6
1.1.3.	Immobilisation methods	6
1.2	Polymers	8
1.2.1.	Polyaniline	12
1.3.	Enzymes	16
1.3.1.	Horseradish Peroxidase	18
1.3.2.	Cytochrome P450	20
1.3.2.1.	Cytochrome P450 _{2D6}	23

1.4.	Serotonin Reuptake Inhibitors	26
1.4.1.	Fluoxetine	26
1.4.2.	Fluvoxamine	27
1.4.3.	Citalopram	27
Chapter 2	Experimental	29
	Introduction	30
2.1.	Materials	31
2.2.	Instrumentation	32
2.3.	Methodology	33
2.3.1.	Electrode surface preparation	33
2.3.2.	Synthesis of polyaniline films onto platinum disk (Pt) or glassy carbon electrode (GCE)	34
2.3.3.	Characterisation of PANI-modified electrode using cyclic voltammetry	35
2.3.4.	Preparation of polyaniline-enzyme electrodes	35
2.3.5.	Electrochemical measurements using HRP-based biosensor	36
2.3.6.	Spectroelectrochemistry (SEC)	38
2.3.7.	Scanning electron microscopy (SEM)	38
2.3.8.	Electrochemical analysis of GC/PANI/CYP2D6 biosensor in the presence of serotonin reuptake inhibitors	39
2.3.9.	Inhibitory studies of GC/PANI/CYP2D6	40

Chapter 3	Results and Discussion	41
	Introduction	42
3.1.1.	Preparation of polyaniline film	43
3.1.2.	CV characterisation of Pt/PANI electrode in 1 M HCl	47
3.1.3.	SWV characterisation of Pt/PANI electrode in phosphate buffer	51
3.2.	Horseradish peroxidase-based biosensor	53
3.2.1.	PANI-mediated electro-catalytic reduction of H ₂ O ₂	53
3.2.1.1.	Square wave voltammetry of Pt/PANI/HRP biosensor	55
3.2.1.2.	Cyclic voltammetry of Pt/PANI/HRP biosensor	57
3.2.2.	Spectroelectrochemistry (SEC)	63
3.2.3.	Scanning electron microscopy Analysis (SEM)	64
3.3.	Cytochrome P450 _{2D6} -based biosensor	67
3.3.1.	CV analysis of fluoxetine metabolism by GC/PANI/CYP2D6 biosensor	68
3.3.2.	DPV analysis of fluoxetine metabolism by CYP2D6 biosensor	70
3.3.3.	Other SRIs analysis by GC/PANI/CYP2D6 biosensor	77
3.3.4.	Analysis of bufuralol using CYP2D6 biosensor	79
3.3.5.	Inhibition of CYP2D6 by quinidine	82
	Conclusion	85
	References	87

LIST OF FIGURES

Figure 1.1:	Main components of a biosensor	7
Figure 1.2:	The polymers of interest in our study	9
Figure 1.3:	Some of the reactions catalysed by CYP2D6	25
Figure 1.4:	Typical catalytic cycle of a substrate by a CYP450	28
Figure 3.1:	Cyclic voltammograms of electropolymerisation of PANI on Pt disk electrode at different scan rates in a solution containing 0.2 M aniline/1 M HCl	44
Figure 3.2:	Electrosynthesis of PANI film on a $1.77 \times 10^{-2} \text{ cm}^2$ Pt disk electrode at 100 mV s^{-1} in a solution containing 0.2 M aniline/1 M HCl	45
Figure 3.3:	Multi-scan cyclic voltammogram of Pt/PANI electrode in 1 M HCl	48
Figure 3.4:	The plots of the (a) dependence of peak currents on potential scan rate and (b) peak currents as a function of the square root of the potential scan rate for Pt/PANI electrode	49
Figure 3.5:	Net cathodic square wave voltammograms of the Pt/PANI/HRP electrode at different amplitudes in buffer solution	52
Figure 3.6:	Square wave voltammetric responses of Pt/PANI/HRP biosensor to different $[\text{H}_2\text{O}_2]$ in argon-degassed phosphate buffer	56
Figure 3.7.1:	Voltammetric responses of Pt/PANI/HRP biosensor at low peroxide concentration	58

Figure 3.7.2: Cyclic voltammograms of Pt/PANI/HRP biosensor in the presence of different concentrations of H_2O_2 at 5 mV s^{-1}	59
Figure 3.7.3: Calibration curve obtained with Pt/PANI/HRP biosensor for different $[\text{H}_2\text{O}_2]$ against peak current	61
Figure 3.8: SEM images of screen-printed electrodes	66
Figure 3.9: CV responses of GC/PANI/CYP2D6 biosensor to different concentrations of fluoxetine	69
Figure 3.10.1: DPV responses of CYP2D6-based biosensor to fluoxetine	72
Figure 3.10.2: A plot of current against different concentrations of fluoxetine at a scan rate of 20 mV s^{-1}	73
Figure 3.10.3: Linear range of CYP2D6 biosensor in the presence of fluoxetine in buffer solution	74
Figure 3.11: Catalysis reaction for CYP2D6 N-demethylation of fluoxetine at the polyaniline-modified electrode	76
Figure 3.12: Voltammetric responses of CYP2D6 to fluvoxamine at a scan rate of 10 mV s^{-1}	78
Figure 3.13.1: Voltammetric responses of GC/PANI/CYP2D6 biosensor to bufuralol at 10 mV s^{-1}	80
Figure 3.13.2: Response curve of the CYP2D6-based biosensor to different concentrations of bufuralol and linear range calibration	81
Figure 3.14: Voltammetric responses of GC/PANI/CYP2D6 biosensor to bufuralol, fluoxetine and quinidine at 10 mV s^{-1}	83

LIST OF TABLES

Table 1.1:	Some electronically conducting polymers	11
Table 1.2:	Different forms and colours of polyaniline (PANI)	15
Table 1.3:	Different groups of enzymes	17
Table 1.4:	Substrates and inhibitors of some human CYP isoenzymes	22



Chapter 1: Literature Review



INTRODUCTION

Since the first demonstration by Clark and Lyons, [1] that an enzyme could be integrated into an electrode to form a “biosensor”, the development of such devices has made considerable progress [2]. Over the past two decades a tremendous amount of activity in this area has been witnessed [3]. According to Turner, a biosensor is “a device incorporating a biological sensing element either intimately connected to or integrated within a transducer.”

The focus of this study is on the electrochemical synthesis and characterisation of polyaniline-modified electrodes. These electrodes were then used in the fabrication of enzyme-based biosensors. The fabrication of horseradish peroxidase-based (HRP) biosensor for monitoring hydrogen peroxide in an aqueous medium was investigated. The second application of this PANI-modified electrode focused on the fabrication of cytochrome P450_{2D6}-based (CYP2D6) biosensor.

It must be emphasised here that HRP enzyme was used in the study for method development because is more robust in nature and cheaper than CYP2D6.

1.1. BIOSENSORS

According to Turner's definition, it is clear that a biosensor have two principal components: a molecular recognition element (the biological component) and a signal-generating or the instrumental component (a transducer). Biosensors combine the exquisite selectivity of biology with the processing power of modern electronics. The major processes involved in any biosensor system are analyte recognition, signal transduction and read-out.

A simple, general schematic of a typical biosensor is shown in Figure 1.1.

1.1.1. BIOLOGICAL COMPONENT

The biological component could be an enzyme, antibody, nucleic acid, receptor, microorganism, whole cell or tissue, and serves to selectively catalyze a reaction or facilitate a binding event. Biological molecules, which are in intimate association with the physicochemical transducer can selectively recognize target analyte(s), for example, glucose oxidase has the potential to selectively recognise glucose [4-5]. Biosensors can be classified based on the biological component used.

Nucleic acid biosensors are based on affinity reactions involving DNA molecules [6] and one of the potentially major applications of these biosensors is for the testing of bacterial contamination of food, water, plant and soil samples [7-9] as well as for the diagnosis of human diseases related to gene mutations or pathogenic microorganisms [3,10].

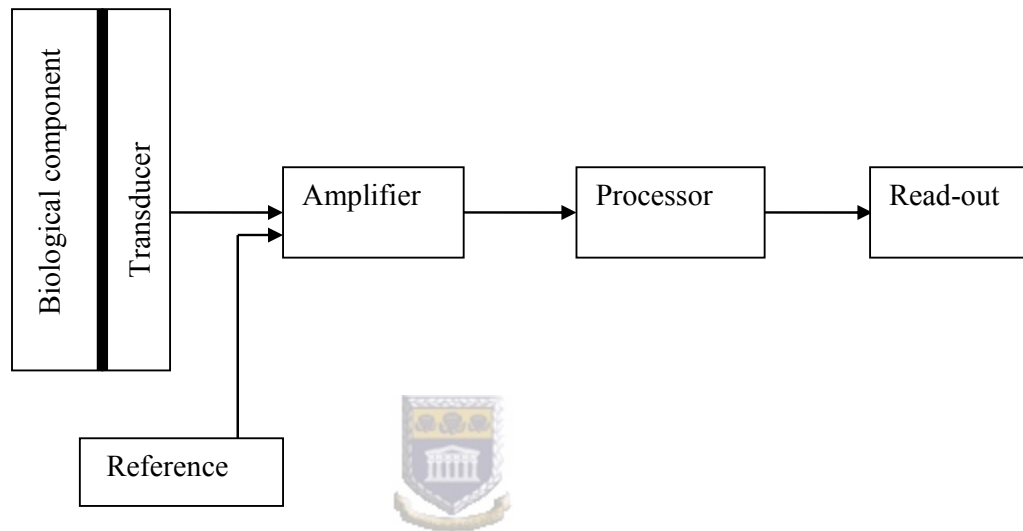


Figure 1.1: Main components of a biosensor.

The biological component converts the substrate into a product. This reaction is determined by the transducer, which converts it into an electrical signal. The output from the transducer is amplified, processed and displaced.

Biosensors using microorganisms are known as microbial biosensors. These biosensors exploit the metabolic functions of living microorganisms to effect detection and measurements of the analyte. These microbial biosensors can either measure oxygen consumption or production of acid wastes resulting from metabolic activities of microorganism [11-13].

Immunosensors are biosensors that use antibodies or antigens as their sensing elements [14] and are based on the highly specific interaction between antibody and its corresponding antigen. Immunosensors have been constructed for a single analyte determination or for a group of analytes (multi-analyte) in the same sample [15-17].

Tissue and cell materials of both plants and animals have also been employed in the fabrication of biosensors. The use of tissue and cell materials is very attractive because the enzymatic pathways are maintained in their natural environment and result in a considerable stabilization of the desired high enzyme activity [18-19].

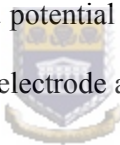
Enzymes are the first biological components to be used in biosensors, and remain by far the most widely used and the best understood in biosensor technology. The most widespread and successful biosensor is based on the enzyme, glucose oxidase for monitoring glucose [4-5, 20-21]. Other enzymes that have also been studied include alcohol oxidase [22], cholinesterase [23], cytochrome P450 [24-28] and horseradish peroxidase (HRP) [29-33].

1.1.2. TRANSDUCERS

The transducer is the key part of a biosensor and its purpose is to convert the biological recognition event into a useful electrical signal. Transducers can take many forms depending on the parameters being measured, for example electrochemical, optical [34] or field effect transistors [35]. Again biosensors can be classified based on the transducer being used.

Electrochemical biosensors have received most attention in biosensing development [3] and they are further divided into coulometric, potentiometric and amperometric biosensors.

In potentiometric biosensors, the analytical information is obtained by converting the biorecognition process into a potential signal, which in reality is the potential difference between the indicator electrode and the reference electrode [12-13, 36].



Amperometric biosensors are based on monitoring the current on the working electrode, associated with oxidation or reduction of an electroactive species involved in the recognition process. Amperometric techniques are linearly dependent on analyte concentration and give a normal dynamic range [37]. These types of biosensors are the most attractive of the electrochemical biosensors because of their high sensitivity and wide linear range [3].

1.1.3. IMMOBILISATION METHODS

The essential task in construction of any viable biosensor is to efficiently and effectively attach the biological component onto the transducer. This process is

known as immobilisation. The selectivity, the long-term stability and the reliability of a biosensor are dependent on the biochemical recognition elements being closely fixed to the surface of the transducer in question [3, 36].

Several methods can be used for immobilising the biological material onto the transducer, including entrapment in a polymer film [20, 38-39], covalent binding [40] and cross-linking [41].

Electrostatic adsorption involves the electropolymerisation of the polymer on the electrode. Biological components are then electrostatically attached onto the surface of an electroactive polymer by application of an oxidizing or reducing potential. This effective biosensor format has examined the amperometric behavior of immobilised horseradish peroxidase (HRP) in polyaniline [42-44] in a polyvinylferrocenium (PVF) film [45] and in multilayer films containing quarternized poly(4-vinylpyridine) (QPVP) [46]. This method of immobilization has been extended to develop rapid, single-step separation-free immunosensors for real-time monitoring of biotin [47].

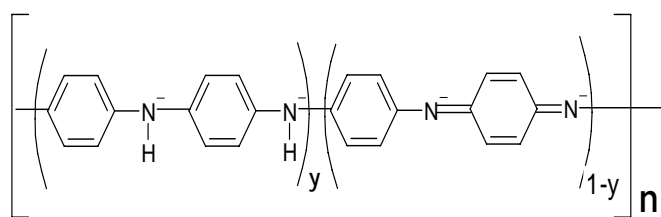
Biosensors have found increased applications in the pharmaceutical, health care (clinical analysis and diagnosis), food industries, environmental monitoring, agriculture and defense.

1.2. POLYMERS

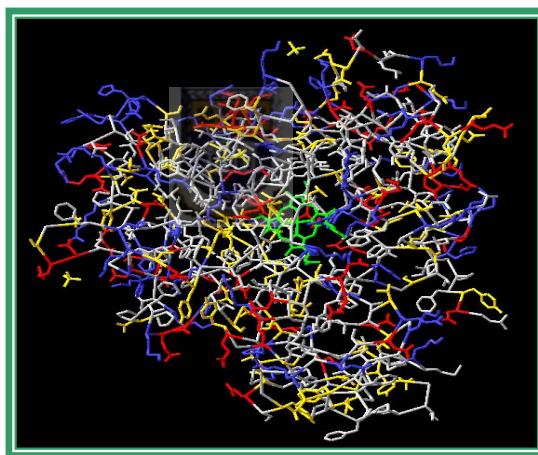
Organic conducting polymers have recently attracted interest because they exhibit a wide range of novel electrochemical properties [48-50]. Of interest to this work are two types of polymers: conducting electroactive polyaniline formed from aniline repeat units and natural polymers that are bioactive enzymes formed from amino acid repeat units Figure 1.2.

According to Lyons conducting electroactive polymers are generally classified under the three major types; redox polymers, ion-exchange polymers (ionomers) and electronically conducting polymers. Redox polymers are defined as conductors containing redox active groups covalently bonded to a non-electroactive polymer backbone, for example poly(vinyl ferrocene). Conduction in these polymers is via electron hopping and they are only conducting over a narrow potential range.





(a)



(b)

Figure 1.2: The polymers of interest in our study: (a) polyaniline and (b) cytochrome P450

Ionomers are ion exchange polymers in which redox active sites are electrostatically incorporated with the redox active component being a counter anion to a polymeric material. Conduction in ionomers is possible either through local electron hopping between fixed redox sites or through physical diffusion of the incorporated redox moiety followed by electron transfer.

Electronically conducting polymers are different from redox polymers and ionomers in that the backbones of these polymers are themselves conducting. Electronically conducting polymers have been known to show transition from insulator to conductor and vice versa as the polymers move from one oxidation state to another and are conductive over an extended potential range. Examples of this type of polymers are shown in Table 1.1. It is thought that the three factors delocalization, doping and morphology contribute to the measured conductivity of an electronically conducting polymer. Of interest in this study is polyaniline, which will be looked further in the next section.

Table 1.1: Some electronically conducting polymers

Polymer	Symbol	Chemical Repeat Unit
Polyacetylene	PAC	-(CH)_x
Polypyrrole	PPy	$\text{-(}\begin{array}{c} \text{C} \\ \text{C} \\ \text{N} \\ \text{H} \end{array}\text{)}_n$
Polythiophene	PTh	$\text{-(}\begin{array}{c} \text{C} \\ \text{C} \\ \text{S} \end{array}\text{)}_n$
Poly(p-phenylene)	PPP	$\text{-(C}_6\text{H}_4\text{)}_n$
Polyaniline	PANI/PANi/ PAn	$\text{-(}\begin{array}{c} \text{C}_6\text{H}_4\text{-N}^+\text{H} \\ \text{C}_6\text{H}_4\text{-N}^+ \end{array}\text{)}_y \text{-(}\begin{array}{c} \text{C}_6\text{H}_4\text{-N}^+ \\ \text{C}_6\text{H}_4\text{-N}^+ \end{array}\text{)}_{1-y}\text{)}_n$

1.2.1. POLYANILINE

Among the most studied electronically conducting polymers is polyaniline (PANI), which has been studied extensively as an important conducting material that possesses interesting electrical, electrochemical and optical properties [51]. It has also generated considerable interest because of the many routes to its production, its chemical stability and ease of redox doping. The continuous growing interest in the study of PANI is caused by these diverse, unique properties and its promising potential in commercial applications. The potential applications of PANI include anti-corrosive coatings [52-53], secondary batteries [54] and electrochromic devices [55] and electrochemical biosensors [42].

Some examples of the innumerable sensors prepared using polyaniline include glucose oxidase-based biosensor [5, 20], cholinesterase-based biosensor [23] and horseradish peroxidase-based biosensors [42-43] and CYP2D6-based biosensor [28].

Advantages of utilizing polyaniline-coated electrodes in biosensors are acceleration of electron transfer reactions, impressive signal amplification and elimination of electrode fouling [56]. This polymer also provides a suitable environment for immobilisation of biological components.

Polymer films can be deposited on electrode surfaces very readily. Polymerisation of the monomer aniline can be achieved by either chemical or electrochemical methods. However, electrochemical synthesis is rapidly becoming the preferred method for preparing electrically conducting polymers because of its simplicity and reproducibility. In both cases, that is, chemical and electrochemical methods,

the polymer is prepared from a dilute monomer solution containing a suitable counter anion that serves as the dopant. The method chosen depend on the form of the polymer required.

Chemical synthesis generally yields a powdered material or solution of low molecular weight oligomers whereas electrochemical synthesis yields an insoluble film on an electrode surface [37].

An important advantage of the electropolymerisation technique in the fabrication of biosensors is that the film thickness and characteristics can be controlled by monitoring polymerisation charge [57], and also the process is localised at the electrode surface. Electropolymerisation also offers an effective route for creating highly controllable size exclusion films [56].



Electrochemically, the polymer can be grown on the electrode surface by pulse [58-59], galvanostatically [58], potentiostatically [28] or potentiodynamically [6,42-43,60].

During galvanostatic method the current is kept constant and the potential is monitored as the set current is applied for a given period of time. The current may be integrated over this period to yield the total charge using Equation 1.1.

$$Q = \int_{t_1}^{t_2} i dt \dots\dots\dots \text{Eq. 1.1}$$

where Q is the total charge passed (C), t is the time (s) and i is the current applied (A).

Potentiostatic method is carried out by keeping the potential constant between the working electrode and the standard reference electrode. The thickness of the film on the electrode can be controlled by the charge consumed during the process [57].

The potentiodynamic method is achieved by cycling the potential of an electrode between two potentials (initial and final potential) such that the film is alternately oxidized and reduced. The cyclic voltammogram is obtained by measuring the current at the working electrode during the potential scan. The reducing or oxidizing strength of an electrode is precisely controlled by the applied potential.

Electrochemical polymerisation of aniline at an electrode surface is a chain growth process that occurs through free radical mechanism [58]. The free radical is the result of electron transfer between the oxidized monomer in solution and the electrified surface of the electrode.

Polyaniline exhibits different forms at different applied voltage and each of these forms has a different colour [61]. Aniline is electrochemically polymerised into the green, conducting form of polyaniline known as emeraldine salt. After the film is synthesised all four forms can be obtained and reversibly interconverted very quickly electrochemically. Table **1.2** shows the different forms of polyaniline and their respective colours.

Table 1.2: Different forms and colours of polyaniline (PANI)

Name or Form	Colour	Comments
Leucoemeraldine	Clear	Fully reduced, insulating
Emeraldine salt	Green	Partially oxidised, protonated conduction
Emeraldine base	Blue	Partially oxidised, insulating
Pernigraniline	Purple	Fully oxidised, insulating



1.3. ENZYMES

Enzymes are biocatalysts involved in the performance of metabolic reactions [36]. They catalyse reactions rapidly and can be selective for one specific substrate or a group of substrates. It is this remarkable specificity that makes enzymatic methods attractive in sensing devices.

Enzymes can be classified into six different groups based on their functions, which is the nature of chemical reaction that they catalyse, Table **1.3**. Horseradish peroxidase (HRP) and cytochrome P450_{2D6} (CYP2D6), the two enzymes that were used in this study both belong to the oxidoreductase group of enzymes.



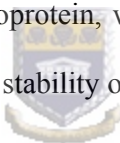
Table 1.3: Different groups of enzymes

Group	Biochemical properties
Oxidoreductases	Catalyse redox reaction by adding or removing hydrogen atoms, oxygen atoms or electrons from one substrate to another.
Transferases	Transfer functional groups between donors.
Hydrolases	Add H ₂ O across a bond, hydrolyzing hydrogen.
Lyases	Add small molecules, for example H ₂ O, NH ₃ or CO ₂ to double bonds or remove these elements to produce double bonds.
Isomerases	Carry out many kinds of isomerisation, for example L to D isomerisation.
Ligases	Catalyse reactions in which two chemical are joined or ligated with the use of energy from ATP, that is, ATP-linked bond formation.

1.3.1. HORSE RADISH PEROXIDASE

Horse radish peroxidase (HRP) is a redox hemoglycoprotein with a molecular weight and isoelectric point of about 42 000 Da and 8.8, respectively. Similar to all peroxidases, it catalyses reactions involving peroxides. Native HRP consists of a polypeptide chain containing 308 amino acid residues.

HRP contains a single iron (III) protoporphyrin IX prosthetic group in which the iron centre has six coordination positions. Four of these coordination positions are occupied by porphyrin nitrogen atoms, the fifth by a protein group, histidine. Various compounds can occupy the sixth position, and it is in this position that the peroxidase exchange substrate. The porphyrin is held in place by electrostatic interactions between the propionic side chain of the haem and lysine molecule in the apoprotein. HRP is a metalloprotein, where calcium appears to play a major role in maintaining the structural stability of the enzyme.



HRP has been widely applied in mono-enzyme biosensors for detection of hydrogen peroxides and organic peroxides [43, 62-63], in bi-enzyme biosensors for detection of substrates such as alcohol, choline and lactate [22, 40-41]. It has also been applied in fabrication of organic-phase biosensors [29, 64-65] and in the detection of HRP inhibitors [66-68].

HRP can react with H_2O_2 to form a powerful enzymatic oxidising agent known as compound I (HRP-I), which is a two-equivalent oxidised form containing an oxyferryl heme ($\text{Fe}^{4+}=\text{O}$) and a porphyrin π cation radical. Compound I is catalytically active and can abstract one electron from the substrate to form a

second intermediate, called compound II (HRP-II), which is subsequently reduced back to the HRP resting state, by accepting an additional electron from the substrate. The principle of the determination of the response current is based on the reduction of HRP-I and HRP-II formed during the enzyme-catalysed reaction [43].



1.3.2. CYTOCHROME P450

The cytochrome P450 (P450s, CYP450s), family constitutes a superfamily of haem-thiolate monooxygenase enzymes, that has been much studied over the last 30 years. The enzymes catalyse the hydroxylation, or more correctly oxygen atom insertion, of their substrates [69]. They are called cytochrome P450 because of their absorption maximum around 450 nm. These enzymes are widely distributed in bacteria, fungi, plants and animals.

Cytochrome P450s are classified into three categories depending on their distribution: 1) bacterial-type P450s, 2) microsomal-type P450s and 3) mitochondrial-type P450s. The former one is water-soluble protein whereas the last two are membrane-bound proteins. In humans, P450s are located in mitochondria and endoplasmic reticulum with highest concentration in hepatocytes (liver cells), and can also be found in the intestines, lungs and other organs.

Cytochrome P450 enzymes are a superfamily of similar proteins (isoenzymes) with the same porphyrin-haem complex as the catalytic center but different amino acid sequences, altering the topography of the active site.

The P450 proteins are categorised into families and subfamilies by the sequence similarities. Sequences that are greater than 40 % identical at the amino acid level belong to the same family and those that are greater than 55 % identical are placed in the same subfamily. There are more than 2500 cytochrome P450 sequences known. Humans have 18 families of cytochrome P450 genes and 43 subfamilies [70].

Literature indicates that there are six major forms of CYP450 isoenzymes that are involved in the metabolism of pharmaceuticals in man, and these are: CYP1A2, CYP2D6, CYP2C9, CYP2C19, CYP3A4 and CYP2E1 [71]. Some known substrates and inhibitors of these isoenzymes are listed in Table 1.4.

The widespread interest in the P450s is justified by the enormous range of physiological processes involving enzymes from this family. These include, but are not limited to, steroid metabolism, drug deactivation and procarcinogen activation.

Cytochrome P450 enzymes are also involved in metabolism of a plethora of both exogenous and endogenous compounds. This is an initial step in biotransformation and elimination of a wide variety of drugs and environmental pollutants. The primary physiological role of these enzymes in drug metabolism is that of physiological clearance, by conversion of the drug into a more hydrophilic metabolite, which is then easily excreted into either urine or bile. One common way of metabolising drugs involves the alteration of functional groups on the parent molecule, for example oxidation via the cytochrome P450 enzymes. The P450 enzymes are the most important enzyme systems involved in phase I of drug metabolism.

Table 1.4: Substrates and inhibitors of some human CYP isoenzymes

CYP ISOENZYME	SUBSTRATES	INHIBITORS
CYP1A2	Caffeine, propranolol, phenacetin	Furafyline
CYP2C9	(S)-Warfarin, diclofenac, ibuprofen	Sulphaphenazole
CYP2D6	Metoprolol, bufuralol, codeine, fluoxetine	Quinidine
CYP2E1	Chlorzoxazone, <i>p</i> -nitrophenol	Diethyldiithiocarbamate
CYP3A4	Erythromycin, midazolam, nifedipine	Ketoconazole

Bacterial cytochrome P450_{cam} from *Pseudomonas putida*, (CYP101 or P450_{cam}) has been one of the most studied P450 enzymes [72]. The CYP101 catalyses the hydroxylation of camphor at the 5-exo position [73-74]. This enzyme can be expressed in *E. coli*, its high-resolution crystal structure is available and its biochemistry is well documented.

1.3.2.1. CYTOCHROME P450_{2D6}

Although cytochrome P450_{2D6}, (CYP2D6) is mainly a hepatic enzyme which constitutes only about 2% of the total CYP protein in the liver [75], it has been shown to contribute significantly towards the metabolism of over 30 prescribed drugs. CYP2D6 has been studied extensively because it is the first human P450 for which genetic polymorphism, was clearly demonstrated [76].

Genetic polymorphism implies that distinct population differences are apparent in enzyme expression or activity due to variations in DNA sequence. These differences in DNA sequence can lead to differences in drug metabolism and clearance for CYP2D6 substrates. Individuals are classified as either poor or extensive (normal) metabolisers. Poor metabolisers do not produce functioning enzyme and are unable to metabolise drugs via this pathway. The PM not only lacks functional CYP2D6 but also have impaired metabolism of more than 70 drugs. They are at risk for drug accumulation and toxicity from drugs metabolized by this isoenzyme. Poor metabolizers of CYP2D6 can exhibit less response to drug therapy compared to normal metabolisers when formation of an active

metabolite is essential for drug action. Approximately 5 to 10 % of the Caucasian population is poor metabolisers.

Extensive metabolisers comprise the rest of the population, with some individuals (ultra rapid metabolisers, URM) producing a lot of CYP2D6 and having a substantial capacity to metabolise via this pathway [77].

CYP2D6 is responsible for the metabolism of antidepressants and neuroleptic drugs. Some of the many reactions that are catalysed by CYP2D6 are shown in Figure 1.3. CYP2D6 has been indicated, as the enzyme responsible for metabolism of the serotonin reuptake inhibitors (SRIs). Examples of SRIs that are metabolised by CYP2D6 are fluoxetine, fluvoxamine, citalopram, paroxetine and sertraline.



The catalytic mechanism of most of the monooxygenation reactions is considered to be relatively general and can be described by the cycle below, Figure 1.4. In this catalytic cycle, introduction of the first electron to a substrate-bound cytochrome P450, in this case CYP2D6 reduces ferric heme to a ferrous form to obtain an oxygen molecule. The second electron introduced to oxygenated heme, resulting in activation of the bound oxygen molecule, and an oxygen atom attaches to the substrate [69].

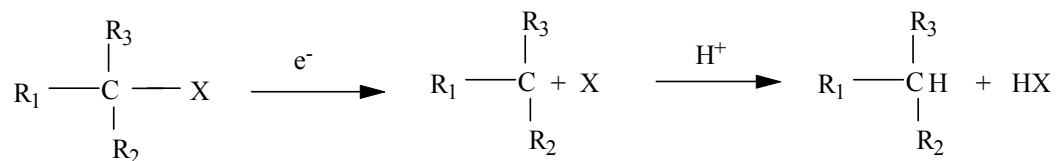
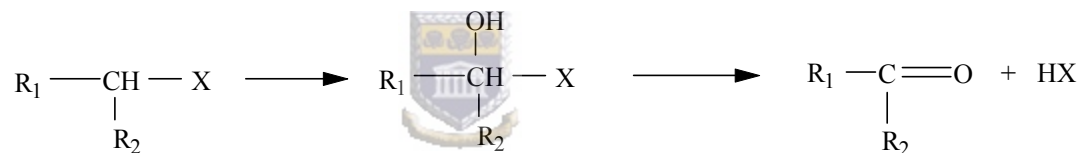
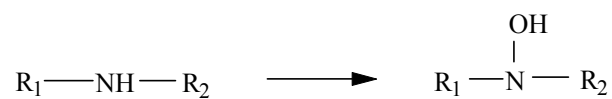
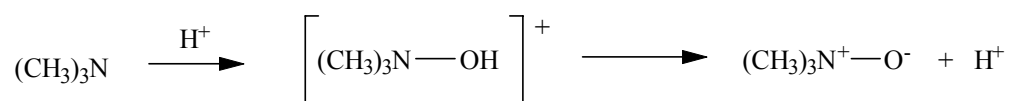
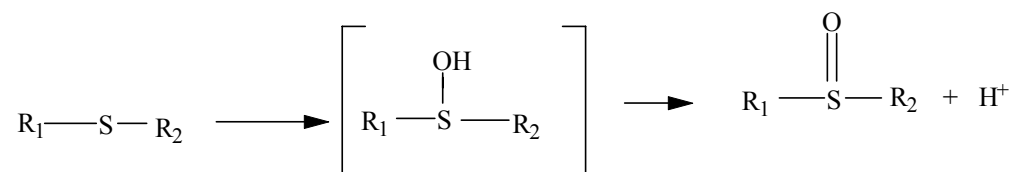


Figure 1.3: Some of the reactions catalysed by CYP2D6

1.4. SEROTONIN REUPTAKE INHIBITORS (SRIs)

Depression is a psychiatric condition in which the neurotransmitter, serotonin is implicated. Currently it has been found that the best treatment of chronic depression is pharmacologic or drug treatment. The continuous demand of new antidepressant drugs with minimal side effects gave rise to the development of serotonin reuptake inhibitors group of drugs. These drugs (SRIs) increased the pharmacological options for the treatment of depression. By enhancing serotonergic transmission and inducing down-regulation of postsynaptic receptors, these agents provide effective antidepressant activity without the sedating, anticholinergic, or cardiotoxic reactions observed with tricyclic antidepressants, (TCAs) [78]. SRIs are also used for the treatment of anxiety, obsessive-compulsive disorder and any other disorder in which serotonin plays a role.



The five serotonin reuptake inhibitors (SRIs), fluoxetine, fluvoxamine, paroxetine, sertraline and citalopram have become the most prescribed antidepressants in many countries [79]. They have similar antidepressant efficacy and a similar side effect profile. However, they differ in their chemical structure, metabolism and pharmacokinetic properties [79-80].

1.4.1. FLUOXETINE

Fluoxetine has been prescribed more than any other antidepressant partly because of its efficacy, benign side effects and treatment in case of overdose. It is administered as a racemic mixture of two enantiomers, *R*- and *S*-enantiomers. Fluoxetine undergoes extensive metabolic conversion, leading to a long acting and

pharmacologically active metabolite, norfluoxetine that has selectivity for serotonin reuptake comparable with that of the parent compound, fluoxetine. Norfluoxetine has a long half life of 7-15 days compared to 1-3 days for fluoxetine. This means that the risk of a drug-drug interaction mediated by this metabolite persists for weeks after fluoxetine has been discontinued because of its long half life. Thus norfluoxetine is likely to contribute substantially to the efficacy and side effect profile of fluoxetine [81]. This is the only metabolite of serotonin reuptake inhibitors that contribute to clinical actions of the drug.

1.4.2. FLUVOXAMINE

Fluvoxamine is the antidepressant drug that belongs to the group of serotonin reuptake inhibitors. Its half life is approximately one day and is metabolised in the liver by CYP450 enzymes (CYP2D6 and CYP1A2) via demethylation and deamination [82]. The metabolite of fluvoxamine are not SRIs, thus they do not contribute to the clinical action of the drug.

1.4.3. CITALOPRAM

Citalopram, like fluoxetine is a racemic mixture and a very potent serotonin reuptake inhibitor. Its half life is approximately one (1) day. Biotransformation occurs by N-demethylation to form a principal metabolite, desmethylcitalopram (DCIT/ DCT) and other metabolites [83-84].

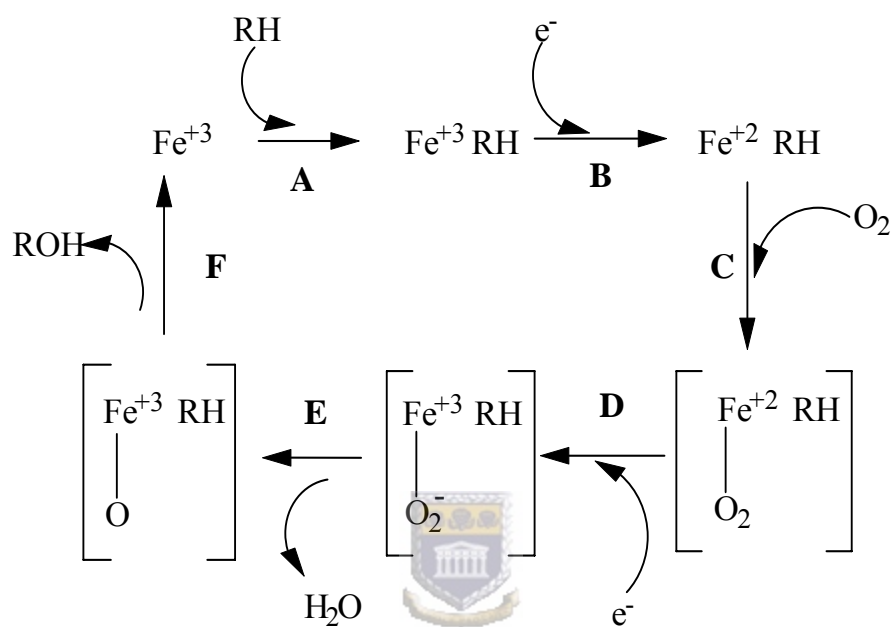


Figure 1.4: Typical catalytic cycle of a substrate by a cytochrome P450

Chapter 2: Experimental



INTRODUCTION

The antidepressants of the group serotonin reuptake inhibitors (SRIs) are currently widely prescribed drugs [79]. They are routinely and effectively dispensed to adults and children in the treatment of major depressive disorders. The side effects in the general population have been found to be benign [80].

Literature suggests that isoforms of the heme-thiolate Cytochrome P450 (CYP450) proteins is indicated in the metabolism of this drug. Specifically the Cytochrome P450_{2D6} (CYP2D6) isoform is responsible for the biotransformation of these drugs [85].

In the present study we investigate an electrochemical method for the detection of SRIs mediated by electroactive polyaniline films. Polyaniline was electrochemically synthesised under potentiodynamic conditions.



2.1. MATERIALS

All chemicals were purchased from Sigma-Aldrich (Cape Town, South Africa) and were of analytical grade. These include enzymes, aniline, hydrogen peroxide, fluoxetine hydrochloride, citalopram hydrobromide, bufuralol, fluvoxamine, quinidine sulphate, sulphuric acid, hydrochloric acid, potassium chloride, disodium hydrogen phosphate and potassium dihydrogen phosphate monohydrate. The enzyme peroxidase, from horseradish (EC 1.11.1.7 Type II, 150-250 units/mg, 42 000 Da) was used for preparation of horseradish peroxidase (HRP)-based amperometric biosensor. One unit of horseradish peroxidase (HRP) forms 1.0 mg purpurogallin from pyrogallol in 20 seconds at pH 6 at 20°C.



Cytochrome P450_{2D6} (CYP2D6, EC 231-791-2, 212 units/mg) was used for fabrication of CYP2D6-based amperometric biosensor. One unit of CYP2D6 converts 1 nanomole of bufuralol into hydroxybufuralol per minute at pH 7.4 at 37°C. Both enzymes were kept in the freezer when not used.

Aniline was distilled under vacuum before being used for electropolymerisation process. The distilled aniline was then kept in the freezer when not used. Substrates for both enzymes were freshly prepared daily. Hydrogen peroxide was used as HRP substrate while bufuralol, citalopram, fluoxetine and fluvoxamine were all used as substrates for CYP2D6. Quinidine, a well known CYP2D6 inhibitor was used for inhibition studies.

Phosphate buffer solutions of different compositions were prepared from anhydrous disodium hydrogen phosphate, potassium dihydrogen phosphate monohydrate and potassium chloride. The anhydrous phosphate salt was dried for 2 hours at 110°C and cooled in a desiccator before being used for buffer preparation. The buffer solutions were 0.05 M (pH 6.8) and 0.05 M, 0.1 M KCl (pH 7.07), for HRP and CYP2D6, respectively.

Analytical grade argon (Afrox, South Africa) was used to degas the system. Concentrated sulphuric acid (H₂SO₄) and hydrochloric acid (HCl) were used as received to prepare 0.2 M H₂SO₄ and 1 M HCl solutions, respectively

2.2. INSTRUMENTATION

All electrochemical experiments were carried out and recorded with a computer interfaced to a BAS 50W integrated automated electrochemical workstation (Bioanalytical Systems, Lafayette, IN, USA).

Electropolymerisation, cyclic voltammetry, square-wave voltammetry and differential pulse voltammetry were carried out in either 10 ml or 20 ml electrochemical cell placed in a Faraday cage (BAS C2), with Ag/AgCl (3 M NaCl type) purchased from BAS as reference electrode for all electrochemical studies.

Platinum disk, glassy carbon electrode (GCE), and screen-printed carbon electrodes (SPCEs) were used as working electrodes. The Pt disk ($1.77 \times 10^{-2} \text{ cm}^2$) and GCE ($7.1 \times 10^{-2} \text{ cm}^2$) were obtained from BAS. The screen-printed electrodes ($9.0 \times 10^{-2} \text{ cm}^2$) were donated by Dublin City University and their fabrication is described elsewhere [44]. Platinum mesh and platinum wire as counter electrodes

were obtained from Sigma-Aldrich, South Africa. Alumina micropolish and polishing pads (Buehler, IL, USA) were used for the polishing of the working electrodes (Pt and GCE).

UV-Vis absorbance measurements were recorded at room temperature on a UV/VIS 920 spectrometer (GBC Scientific Instruments, Australia) using specially designed quartz cell (designed in-house) with Pt mesh, Pt wire and Ag/AgCl as working, counter and reference electrodes, respectively.

The morphology of the prepared films was studied with Hitachi X650 scanning electron microscope (GBC Scientific Instruments, Australia) using screen-printed carbon electrodes as working electrodes. An accelerating voltage of 15 kV was employed for all scanning electron microscopy (SEM) studies.

2.3. METHODOLOGY



2.3.1. Electrode Surface Preparation

The surface of the working electrodes (Pt and GCE) was prepared for the deposition of polyaniline films using a thorough cleaning process. The Pt or GCE was cleaned by successive polishing with aqueous slurries of 1 μm , 0.3 μm and 0.05 μm alumina polish, respectively and rinsed thoroughly with copious quantities of de-ionised water after each polishing step.

The counter electrode was regularly cleaned before synthesis and in between synthesis and analysis. The method used in cleaning the counter electrode involved first flaming the electrode in a Bunsen burner until white hot, followed

by rinsing with copious quantities of de-ionised water. This pretreatment of the electrodes was employed before each electropolymerisation step.

A three-electrode arrangement was set up with the GCE or Pt disk electrode as the working electrode, platinum mesh as counter electrode and Ag/AgCl as the reference electrode. The working electrode was then subjected to repeated potential scanning in 0.2 M H₂SO₄ in the potential range of between -1.2 V and +1.5 V until the voltammograms obtained were reproducible. The electrode was then thoroughly washed in de-ionised water on removal from the anodic cleaning solution. Cleaned electrodes were then used directly for polyaniline film deposition.

2.3.2. *Synthesis of Polyaniline Films onto Platinum Disk (Pt) or Glassy Carbon Electrodes (GCE)*



A three electrode arrangement was set up in a sealed 20 ml electrochemical cell. Polyaniline (PANI) films were prepared by electropolymerisation from a 0.2 M aniline solution dissolved in 1 M hydrochloric acid (HCl) solution onto the previously cleaned working electrode. The aniline/HCl solution was first degassed by passing argon through the solution for ten minutes and keeping the argon blanket during electrosynthesis. During the potentiodynamic electrosynthesis, the potential was cycled from an initial potential, E_i , of -0.2 V to a switch potential, E_s , of +1.1 V at a scan rate of 100 mV s⁻¹ versus Ag/AgCl as a reference. The deposition process was stopped after 10 voltammetric cycles.

The polyaniline (PANI)-modified electrode was rinsed with de-ionised water and used as the working electrode in subsequent studies. This electrode will be

referred to as either Pt/PANI or GC/PANI for platinum-and glassy carbon-PANI modified electrodes, respectively.

2.3.3. *Characterisation of PANI-Modified Electrode using Cyclic Voltammetry*

The three electrodes arrangement was again set up in a sealed cell containing 1 M hydrochloric acid (HCl) solution. The potentiodynamically synthesised PANI film was first deposited onto the cleaned working electrode (Pt or GCE) as described in Section 2.3.2. above. The PANI-modified electrode was then anodically scanned in 1 M HCl solution from -0.2 V to +1.1 V at different scan rates of 5, 10, 20, 50, 100 and 200 mV s⁻¹. The cyclic voltammetry was performed for one cycle only at these scan rates.



2.3.4. *Preparation of Polyaniline-Enzyme Electrodes*

A potentiodynamically synthesised PANI film was first deposited onto a cleaned Pt disk or glassy carbon electrode as described in Section 2.3.2 above. The freshly prepared, pure PANI film was then reduced at -500 mV against Ag/AgCl in 5 ml (CYP2D6) of argon degassed phosphate buffer solution, pH 7.07, 0.1 M KCl. The reduction of the PANI film was done until a steady state was achieved which took about fifteen minutes to accomplish.

Electrochemical incorporation of the enzyme, CYP2D6 onto the PANI film was carried out next. In this step, 100 µl CYP2D6 was added to the phosphate buffer solution. This enzyme solution was then further degassed by the passage of argon gas for ten minutes. Enzyme immobilisation was achieved by oxidation of the

PANI film in the presence of CYP2D6 at a potential of +650 mV for 20 minutes while maintaining a blanket of argon in the sealed electrochemical cell.

During the oxidation process, the enzyme CYP2D6 was electro-statically attached to the polymer film via ion exchange process. The resulting biosensor will be referred to as GC/PANI/CYP2D6 biosensor. The biosensor was then rinsed with de-ionised water to remove any unbound enzyme and stored in the working buffer solution (0.05 M, 0.1 M KCl) at 4 °C.

The same procedure was followed for the preparation of HRP-based biosensor on the polymer backbone. In this case a 10 ml buffer solution (pH 6.8) was used and 20 µl of HRP enzyme. The resulting biosensor, Pt/PANI/HRP bioelectrode was stored in the working buffer solution of appropriate pH at 4 °C when not in use.



2.3.5. *Electrochemical Measurements Using HRP-Based Biosensor*

HRP-based biosensor was used in this study for method development because of its robust nature and for being cheap compared to CYP2D6. The HRP-based biosensor was used to monitor the reduction of hydrogen peroxide as the substrate. The cell used for the electrocatalytic reduction of hydrogen peroxide consisted of Pt/PANI/HRP electrode, platinum mesh and Ag/AgCl as the working, counter and reference electrode, respectively.

The 10 ml test solution containing 0.05 M phosphate buffer (pH 6.8) was degassed with argon before any substrate was added and after each addition of small amounts of 0.1 M H₂O₂.

Cyclic, square wave and differential pulse voltammetry were all used to measure the responses of the HRP-based biosensor towards H₂O₂.

Cyclic voltammetry at a slow scan rate of 5 mVs^{-1} was used to study the catalytic reduction of H_2O_2 by the immobilised enzyme between initial and final potential of $+350 \text{ mV}$ and -650 mV , respectively. The cyclic voltammogram of Pt/PANI/HRP in the absence of hydrogen peroxide as a substrate was performed in the working buffer solution, within the same potential range of $+350 \text{ mV}$ and -650 mV . Different volumes of $0.1 \text{ M H}_2\text{O}_2$ were then added to a 10 ml cell containing phosphate buffer ($\text{pH } 6.8$) solution, degassed with argon gas and a blanket of the argon gas kept for the duration of the experiment. The phosphate buffer solution was stirred after each addition of hydrogen peroxide. This was done to ensure homogeneity of the solution before measurements were taken.

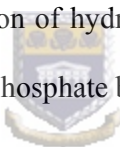
Osteryoung-type square wave voltammetry was also performed with the HRP-based biosensor in phosphate buffer ($\text{pH } 6.8$) containing different concentrations of hydrogen peroxide as the substrate under anaerobic conditions (degassed for 10 minutes and the system kept under an argon blanket). This was done in a reductive direction only (cathodic mode) between $+1.0 \text{ V}$ and -1.0 V . The experimental conditions were: step potential of 4 mV , a frequency of 5 Hz and square wave amplitude of 50 mV .

Differential pulse voltammetry for the reduction wave was also performed in the same potential range of $+1.0 \text{ V}$ and -1.0 V , as in square wave voltammetry. The scan rate used was 20 mV s^{-1} , with pulse amplitude of 50 mV . The sample width, pulse width and pulse period were 17 ms , 50 ms and 200 ms , respectively. The solution was 0.05 M phosphate buffer containing different concentrations of

H₂O₂. The DP voltammetry was performed in both the absence and presence of hydrogen peroxide as the substrate.

2.3.6. Spectroelectrochemistry (SEC)

An optically transparent thin layer electrode (OTTLE) consisted of a piece of Pt mesh as a working electrode, contained in specially designed quartz cell containing the Ag/AgCl and Pt wire as a reference and a counter electrode, respectively. The perforations in the platinum mesh were of such a size that the OTTLE transmitted sufficient visible light, whilst the electrode could still behave essentially as though it was planar. PANI was immobilised on this Pt mesh according to Section 2.3.2 to fabricate a Pt/PANI electrode. This electrode was then used to monitor the reduction of hydrogen peroxide in the presence of HRP (0.08 g l⁻¹) in a bulk solution of phosphate buffer, pH 6.8.



2.3.7. Scanning Electron Microscopy (SEM)

Scanning electron microscopy (SEM) was used to study the morphology of the prepared polyaniline film in the absence and presence of both the enzyme, HRP and substrate, H₂O₂. A three electrode arrangement was set up in which the screen-printed carbon electrodes were used as working electrodes in this study, with the Pt wire and Ag/AgCl as the counter and reference electrode, respectively. The same procedure as stated in Section 2.3.2 and 2.3.4 was followed for electropolymerisation of PANI and immobilisation of the enzyme on the electrode, respectively.

2.3.8. Electrochemical Analysis of GC/PANI/CYP2D6 Biosensor in the Presence of Serotonin Reuptake Inhibitors

The working solution contained argon degassed 0.05 M phosphate buffer (0.1 M KCl, pH 7.07) to which varying concentrations of fluoxetine, as serotonin reuptake inhibitor was added. A standard three electrode arrangement was set up with the freshly prepared GC/PANI/CYP2D6 biosensor set as the working electrode. A cleaned platinum mesh was used as the counter electrode and an Ag/AgCl was used as the reference electrode. The potential scan range was between +1.0 V and -1.0 V and the scan rate used was 10 mV s^{-1} . The buffer solution was not degassed before or after addition of the substrate.



Differential pulse voltammetry experiments were also performed on CYP2D6-based amperometric biosensor in phosphate buffer in both the absence and the presence of fluoxetine. The experimental conditions were as follows: scan rate 20 mVs^{-1} ; pulse amplitude 50 mV; sample width of 17 ms; pulse width of 50 ms; and pulse period of 200 ms. The potential was scanned both cathodically (+0.6 V to -0.8 V) and anodically (-0.8 V to +0.6 V). The DP voltammograms were also recorded under oxygen-saturated conditions.

Fluvoxamine, citalopram and bufuralol were all analysed in a phosphate buffer solution that was not degassed before and after addition of the substrate. For each substrate analysis, a fresh CYP2D6-based biosensor was prepared and used when required. These substrates (fluvoxamine, citalopram and bufuralol) and quinidine

as an inhibitor were studied by cyclic voltammetry technique only. The potential was cycled from an initial potential of +1.0 V to a final potential of -1.0 V. All the experiments were carried out at 10 mVs^{-1} in oxygen-saturated buffer solution (pH 7.07, 0.1 M KCl).

2.3.9. Inhibitory Studies of GC/PANI/CYP2D6

A new biosensor as described in Section 2.3.2 and 2.3.4 was prepared. This was used to study the inhibition of CYP2D6 by quinidine, which is a well known inhibitor of the enzyme. A specific concentration of quinidine was used with a varying concentration of fluoxetine as a substrate.

The three electrode arrangement was still used with GC/PANI/CYP2D6 as a working electrode, platinum mesh as a counter electrode and Ag/AgCl as a reference electrode.



Chapter 3: Results and Discussion



INTRODUCTION

This chapter represents the preparation and analysis of Pt/PANI/HRP and GC/PANI/CYP2D6 biosensors, both prepared from potentiodynamically electropolymerised polyaniline films. The experimental results were analysed under two main headings. The first was the electropolymerisation and characterisation of the polyaniline thin film on both platinum disk and glassy carbon electrodes, in the absence of any enzymes.

Advantages of the electrochemical synthesis of conducting polymer films like polyaniline are (i) an easy one step preparation procedure, (ii) accurate control of the polymer thickness via the electrical charge passed during the film formation process, (iii) localisation of the electrochemical reaction on the electrode surface and (iv) the possibility to build up multi-layer structures.

The second focuses on the use of these PANI films for the construction of biosensors that incorporate either horseradish peroxidase (HRP) or cytochrome P450_{2D6} (CYP2D6).

The HRP-based biosensor, which was used for electro-catalytic reduction of hydrogen peroxide, is used in this study as a model for method development because is cheap and of its robust nature compared to CYP2D6.

The CYP2D6-based biosensor was used for monitoring serotonin reuptake inhibitors (fluoxetine, fluvoxamine and citalopram), bufuralol and for inhibition studies by quinidine.

3.1.1. Preparation of Polyaniline Film

Polyaniline was electrochemically synthesised from the acidic medium of aniline monomer as described in Section 2.3.2. The PANI electrosynthetic films were grown on either platinum disk (Pt) or glassy carbon electrode (GCE) at various scan rates to establish the optimum potential scan rate value, v for producing a homogenous film characterised by high sensitivity, high conductivity and fast electron transfer rates. While chemical oxidation of aniline produces PANI in powder form, electrochemical oxidation in an acidic medium by either galvanostatic, potentiostatic, pulse or potentiodynamic methods produce a film of PANI with a strong adherence to the electrode surface [58].

The following scan rates were investigated 10, 20, 50, 100, 200 and 500 mV s^{-1} . The cyclic voltammograms, CVs, of PANI grown on platinum disk electrode at 50, 100, 200 and 500 mV s^{-1} are shown in Figure 3.1. The CVs presented are recorded after the 10th voltammetric cycle and they are comparable to the CVs of glassy carbon electrode, not shown. It is clear from the CVs that PANI film grown at 50 and 100 mV s^{-1} scan rates, exhibit similarities in the magnitude of their polymerisation currents. The polymerisation currents of PANI films grown at 10 and 20 mV s^{-1} were lower than the one shown in Figure 3.1.

Polyaniline was electrochemically synthesised from an acidic medium of aniline by scanning the potential from -200 mV to +1100 mV at 100 mV s^{-1} . Figure 3.2 shows a typical voltammogram of platinum in 0.2 M aniline/1 M HCl solution for this electropolymerisation process.

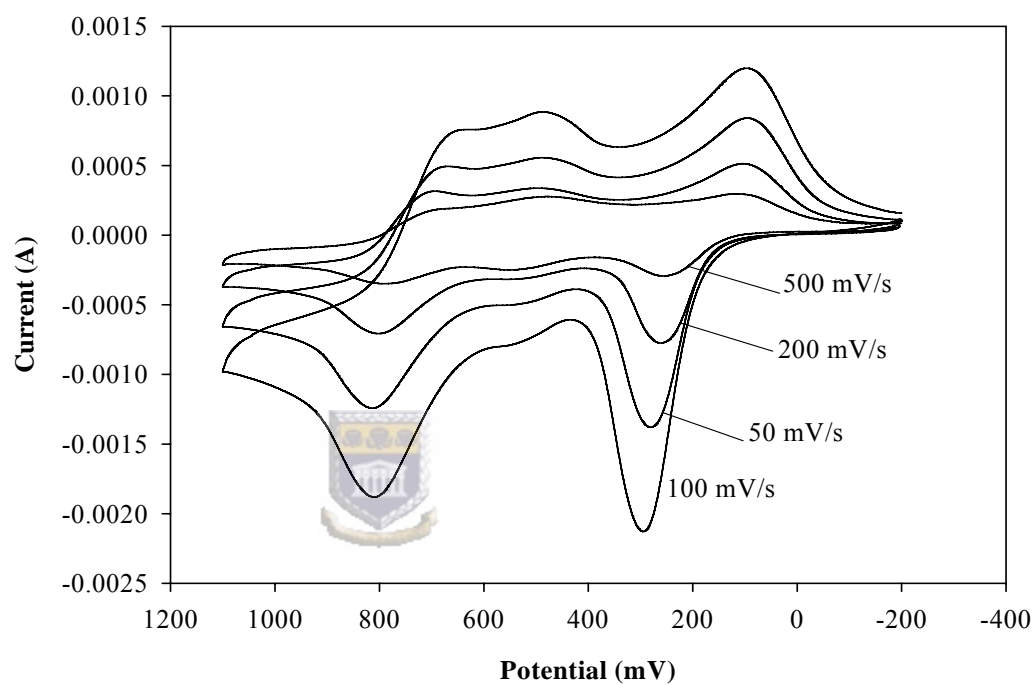


Figure 3.1: Cyclic voltammograms of electropolymerisation of PANI on Pt disk electrode at different scan rates, in a solution containing 0.2 M aniline/1 M HCl.

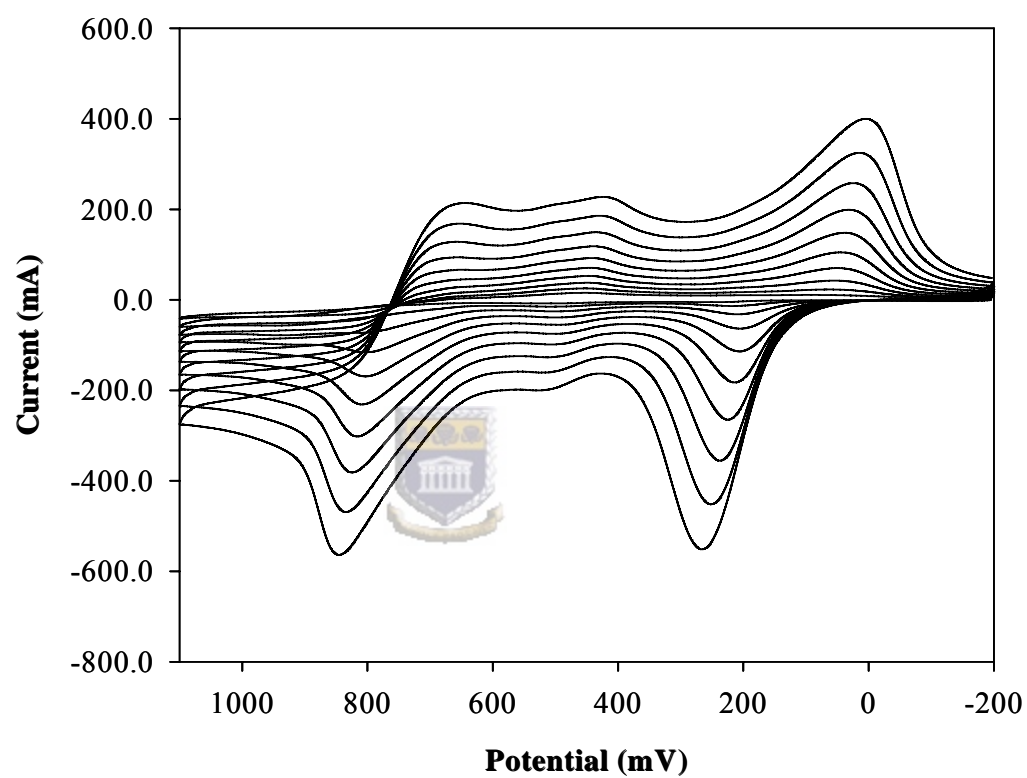


Figure 3.2: Electrosynthesis of polyaniline film on a $1.77 \times 10^{-2} \text{ cm}^2$ Pt disk electrode at 100 mV s^{-1} in a solution containing 0.2 M aniline/1 M HCl.

The nature of growth rate of PANI on Pt electrode is comparable to that reported in the literature [5,42,58,60]. The PANI layer was seen to be redox active in the potential region studied, exhibiting three rapid, reversible and clearly defined pairs of redox peaks. Initially, oxidation of aniline occurred at approximately +900 mV resulting in the nucleation of PANI. During subsequent scans, the oxidation of aniline occurred at lower potentials due to the catalytic effect of PANI, which resulted in deposition of polymer on the electrode surface.

Redox couples A/B and E/F were attributed to the intrinsic processes of the polymer itself. The redox couple A/B occurred at approximately +200 mV and is attributed to the transformation of PANI from the reduced leucoemeraldine (LE) state to the partly oxidised emeraldine (EM) state. The redox couple E/F at approximately +800 mV, corresponds to the transition of the PANI from the LE state to the pernigraniline (PE) state, and is accompanied by the oxidation of aniline monomer. The redox couple C/D at approximately +500 mV, which is generally attributed to the redox reaction of p-benzoquinone, [5,60] is less intense.

An increase in the amplitude of the redox peaks was observed as a consequence of repeated potential scans, indicative of polymer deposition at both Pt and glassy carbon electrodes and confirmed that the polymer was conducting. This electrosynthesised PANI film served two purposes when applied in these biosensor systems. It behaved as an electron mediator, shuttling electrons between the immobilised enzyme and the electrode surface, and also served as a point of attachment for the protein [42,47].

3.1.2. CV Characterisation of Pt/PANI Electrode in 1 M HCl

Multi-scan rate voltammograms of the PANI-modified Pt electrode in 1 M HCl solution are shown in Figure 3.3. Two distinct sets of peaks, (two anodic peaks and two cathodic peaks) were observed in the cyclic voltammograms. Similar CVs have been reported in the literature [42]. Both peak potentials and corresponding peak currents varied as the scan rate values varied. This shows that the polymer was electroactive and diffusion of electrons was taking place along the polymer chain.

The linear dependence of peak currents of anodic peak I on the scan rate (correlation coefficient, $r^2 = 98.6\%$), indicated that we have a thin film of surface-bound conducting electroactive polymer, undergoing rapid reversible electron transfer reaction, Figure 3.4a. The surface concentration of the PANI film, Γ^*_{PANI} was estimated from a plot of I_p against v in accordance with Brown-Anson model [86] using the equation:

$$I_p/v = (n^2 F^2 A \Gamma^*_{\text{PANI}})/4RT \quad \text{Eq. 3.1}$$

where n represents the number of electrons transferred in the process (2), F is the Faraday constant ($96,584 \text{ C mol}^{-1}$), Γ^*_{PANI} is the surface concentration of PANI film (mol cm^{-2}), A is the surface area of the electrode ($1.77 \times 10^{-2} \text{ cm}^2$), v is the scan rate (V s^{-1}), R is the gas constant ($8.314 \text{ J mol}^{-1} \text{ K}^{-1}$) and T is the absolute temperature of the system (298 K).

From this plot, represented in Figure 3.4a, the surface concentration of PANI film, Γ^*_{PANI} was estimated to be $1.85 \times 10^{-7} \text{ mol cm}^{-2}$.

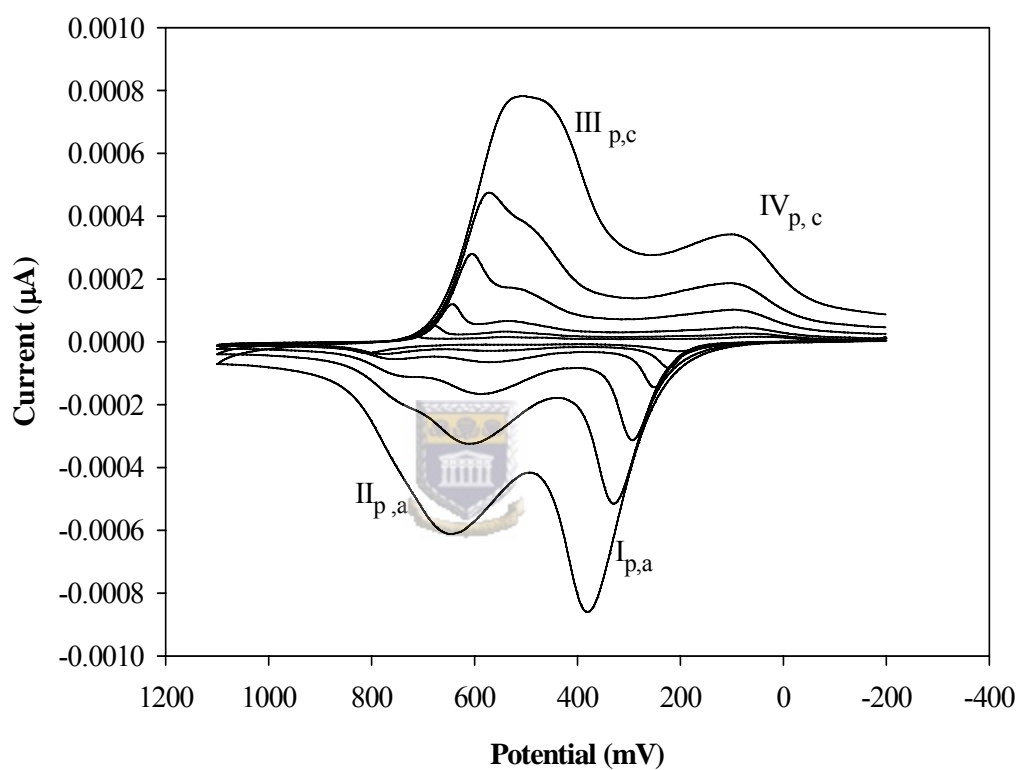


Figure 3.3: Multi-scan cyclic voltammogram of Pt/PANI electrode in 1M HCl.

The peaks were assigned as follows: Peaks $I_{p,a}/IV_{p,c}$ = polyleucoemeraldine radical cation/polyleucoemeraldine.
 Peaks $II_{p,a}/III_{p,c}$ = polyemeraldine/polyemeraldine radical cation. Scan rates: 5, 10, 20, 50, 100 and 200 mV s^{-1} .

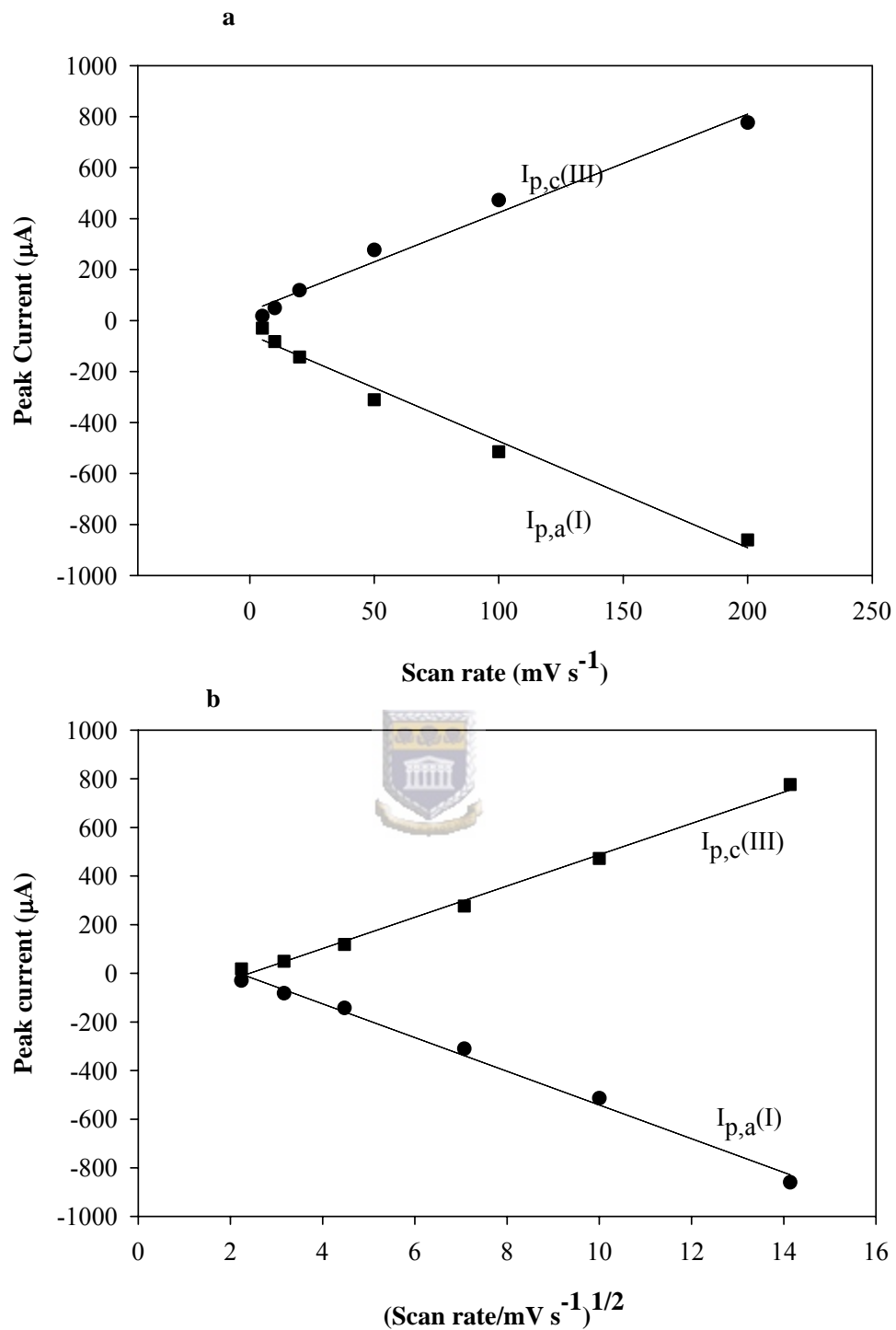


Figure 3.4: The plots of the (a) dependence of the peak currents on potential scan rate and (b) peak currents as a function of the square root of the potential scan rate for Pt/PANI electrode. I_p values were calculated from peaks I and III of the Cvs in Fig. 3.3.

On increasing the scan rate, the magnitude of the peak current increased. However, all the four peak potentials shifted to more positive potentials and became broader. This shows that the currents of the redox species are diffusion-controlled. Since the electroactive polymer is immobilised, the transport/diffusion characteristics of the polymer will be due to electron hopping or delocalization along the polymer chain. Thus the Randel-Sevcík equation [86] may be used to determine the rate of electron transport (i.e. diffusion coefficient of the electrons, D_e), within the polymer, Figure 3.4b.

$$I_{p,c}/v^{1/2} = 0.4463 (nF)^{3/2} A D_e^{1/2} \Gamma_{PANI}^* / L(RT)^{1/2} \quad \text{Eq. 3.2}$$

where L (cm) is the film thickness and the other parameters are the same as in equation 3.1 above.



The PANI film thickness, which was 16.2 nm, was estimated from the voltammetric charge passed during electropolymerisation. The electron diffusion coefficient, D_e calculated from the Randel-Sevcík equation (correlation coefficient, $r^2 = 99.5\%$), was found to be $8.68 \times 10^{-9} \text{ cm}^2 \text{ s}^{-1}$. This compares favourably with literature values [42]. However, Iwuoha *et al.* (1997) reported a D_e value of $6.46 \times 10^{-8} \text{ cm}^2 \text{ s}^{-1}$ for PANI film doped with polyvinyl sulphonate (PVS). Since D_e depends on the conditions used for electrodeposition and on the homogeneity of the film, thus inclusion of the ionic co-polymer polyvinyl sulphonate (PVS) by Iwuoha *et al.* (1997) may have increased the conductivity of the PANI film, resulting in a D_e value approximately one order of magnitude higher than the one reported here.

3.1.3. SWV Characterisation of Pt/PANI Electrode in Phosphate Buffer

Square wave voltammetry was used to examine the peak potentials of the PANI in phosphate buffer, pH 6.8. Figure 3.5 represents the net (difference between forward and reverse currents) SWV responses when the PANI-modified Pt electrode was scanned reductively over a range of amplitudes from 15 to 100 mV, at a frequency of 30 Hz.

A prominent peak at -400 mV was observed and exploited, to monitor electro-catalytic reduction of H_2O_2 at a Pt/PANI/HRP electrode.

Increasing the amplitude resulted in increased currents of this peak. However, increased amplitude was also associated with higher background currents. Therefore, amplitude of 50 mV was then taken for future work as a compromise between these parameters.



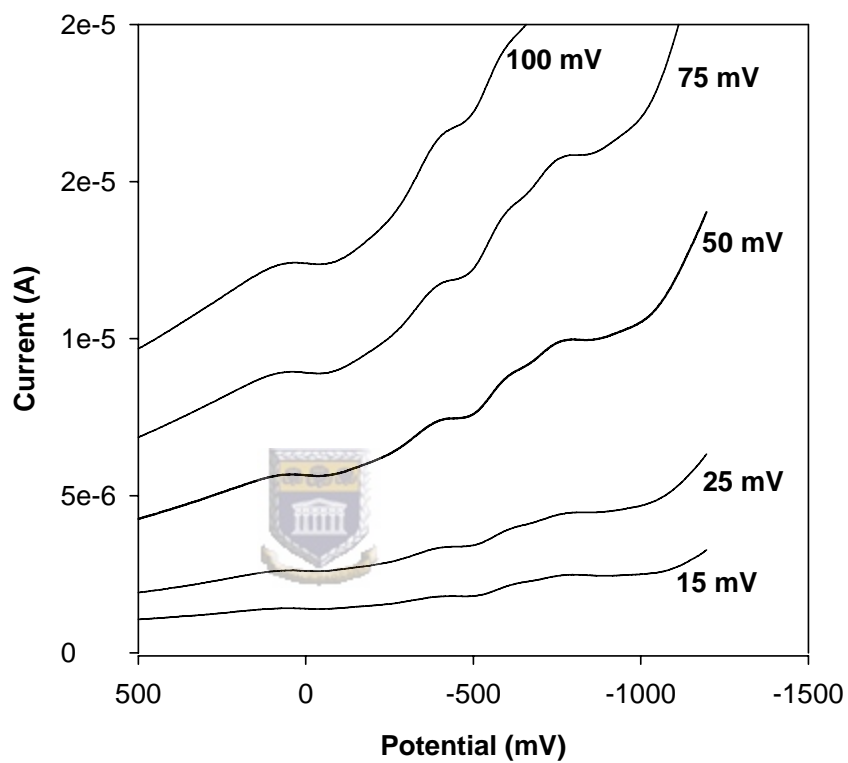


Figure 3.5: Net cathodic square wave voltammograms of the Pt/PANI/HRP electrode performed at 15, 25, 50, 75 and 100 mV in phosphate buffer. Experimental conditions were: frequency 30 Hz and potential step 4 mV.

3.2. Horseradish Peroxidase-Based Biosensor

The horseradish peroxidase-based biosensor was used to develop the method to be used in preparation of cytochrome P450_{2D6}-based biosensor. The HRP enzyme was chosen because of its robust nature and economically cheap. The prepared HRP-based biosensor was used to monitor hydrogen peroxide.

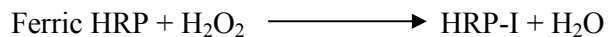
3.2.1. PANI-Mediated Electro-Catalytic Reduction of H_2O_2

Horseradish peroxidase (HRP) was immobilised onto the surface of the polymer by electrostatic interactions with the polymer backbone. This was achieved by applying a potential of +650 mV in the presence of HRP for a period of time (Section 2.3.4).

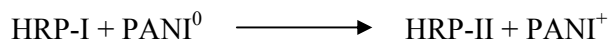
This effective biosensor format facilitated electron transfer between the immobilised enzyme HRP and the electrode surface by the electroactive polymer, PANI, in phosphate buffer of pH 6.8. Without the incorporation of a mediator such as PANI, direct electron transfer between the redox centre of the enzyme and the electrode is known to be slow [87]. Thus appropriate mediators should be selected and used for more efficient electron transfer between HRP and the electrode.

The mechanism of PANI-mediated HRP reduction of H_2O_2 can be presented as follows:

Hydrogen peroxide in solution firstly diffuses to the surface of the film where it is reduced by the immobilised HRP, forming an intermediate spin, iron (IV) compound, known as HRP-I.



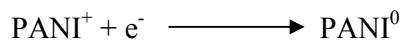
HRP-I also known as Compound I, produced by the enzymatic reaction oxidises PANI to give a low-spin iron (IV) compound known as HRP-II (Compound II). HRP-II is one oxidising equivalent above iron (III) in its resting state.



The HRP resting state, Fe-III is then regenerated via this intermediate of HRP-II, Compound-II.



The oxidised PANI^+ is then electrochemically reduced at the electrode yielding an enhanced reduction current. The magnitude of the reduction current produced by the electrode reaction depends on the bulk concentration of the substrate, H_2O_2 .



Electro-catalytic reduction of H_2O_2 was monitored quantitatively using the peak at -400 mV by both square wave voltammetry and cyclic voltammetry.

3.2.1.1. Square-Wave Voltammetry of Pt/PANI/HRP Biosensor

Square wave responses for electro-catalytic reduction of hydrogen peroxide, H_2O_2 at this Pt/PANI/HRP biosensor can be observed in Figure 3.6. When 1 mM H_2O_2 was added to the phosphate buffer of pH6.8, under diffusion-controlled conditions, an initial increase in the current of the potential peak at -400 mV occurred. This demonstrated effective electro-catalytic reduction of H_2O_2 . Subsequent additions of H_2O_2 to the phosphate buffer solution resulted in both a positive shift in the reduction peak of about +190 mV and an increase in the magnitude of this reduction peak, proportional to H_2O_2 concentration.



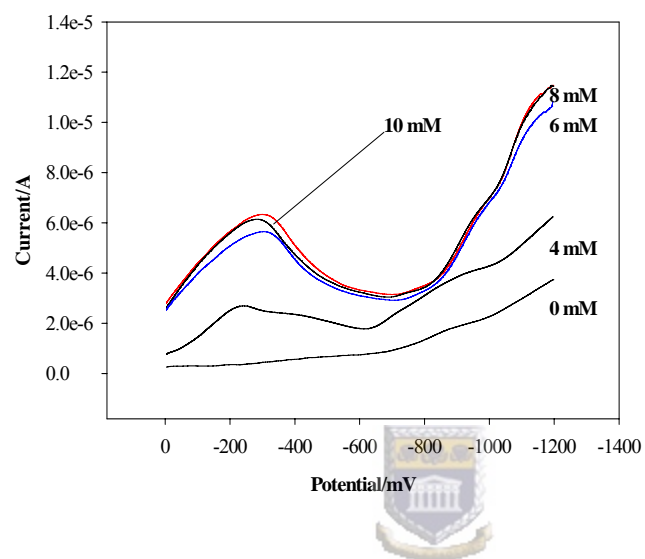


Figure 3.6: Square wave voltammogram of Pt/PANI/HRP in the presence of hydrogen peroxide in a buffer solution. Experimental conditions: step potential of 4 mV, frequency of 5 Hz and amplitude of 50 mV.

3.2.1.2. Cyclic Voltammetry of Pt/PANI/HRP Biosensor

Cyclic voltammetry (CV) was also performed in the absence and presence of hydrogen peroxide. The catalytic current of Pt/PANI/HRP biosensor increases with an increase in the concentration of hydrogen peroxide for measurement carried out at 5 mV s^{-1} . The cyclic voltammogram obtained for the Pt/PANI/HRP biosensor in the absence of peroxide shows two peak potentials at 0 and -400 mV. This represents the electrochemistry of the Pt/PANI/HRP in phosphate buffer solution at 5 mV s^{-1} .

In the presence of hydrogen peroxide, the kinetics of the reaction between H_2O_2 and enzyme (HRP) is coupled to mediator, PANI electrochemistry. However, at low peroxide concentration, for example $20 \text{ }\mu\text{M}$, both enzyme kinetic and electron transfer reaction contributed to the observed peak currents. This resulted in an increase in peak current and a shift in peak potential, Figure **3.7.1**.

However, at high hydrogen peroxide concentrations, for example at concentrations of $500 \text{ }\mu\text{M}$, the enzyme kinetics drives the reaction and the observed voltammetric current is essentially kinetic (catalytic) current. The cyclic voltammograms of Pt/PANI/HRP biosensor was characterised by a plateau (leveling-up) at high reduction potentials, Figure **3.7.2**.

Comparison of the voltammograms with and without H_2O_2 illustrated that the PANI can effectively mediate electron transfer between horseradish peroxidase and platinum electrode surface.

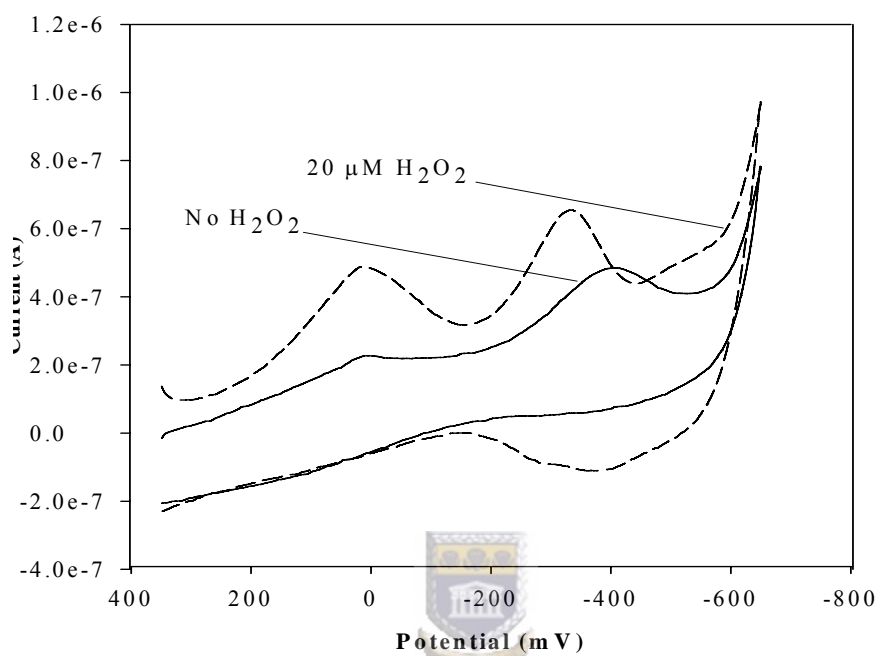


Figure 3.7.1: Voltammetric responses of Pt/PANI/HRP biosensor at low peroxide concentration. Experimental conditions were phosphate buffer and a scan rate of 5 mV s^{-1} .

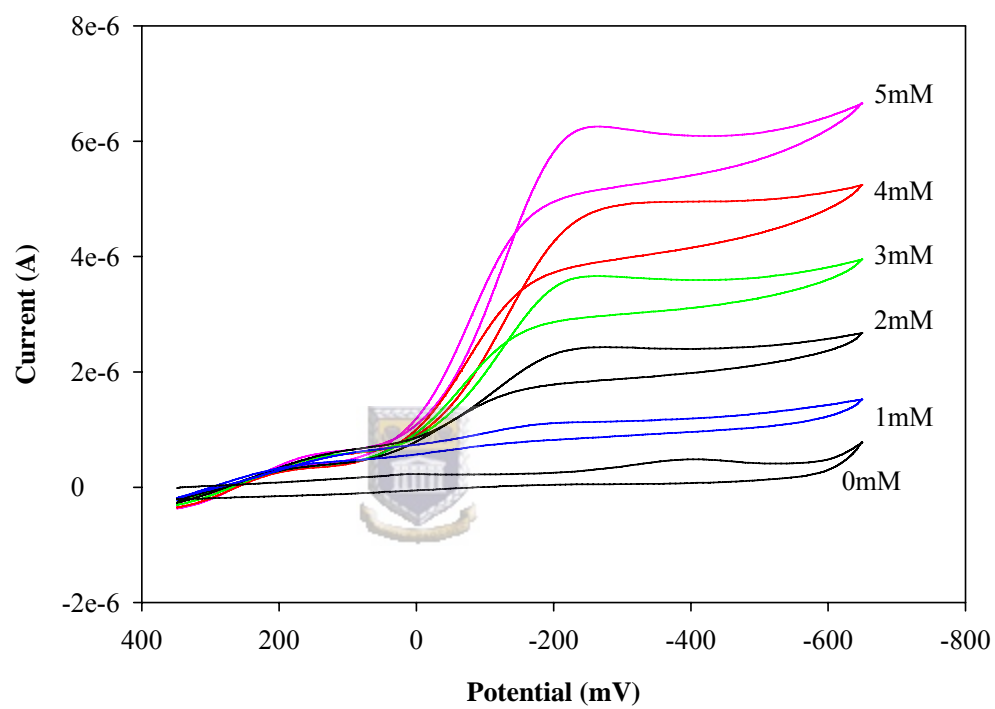


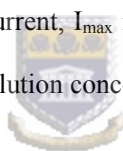
Figure 3.7.2: Cyclic voltammograms of Pt/PANI/HRP biosensor in the presence of different concentrations of H₂O₂. Experimental conditions were phosphate buffer (pH 6.8) and scan rate of 5 mV s⁻¹.

Cyclic voltammetry data was further used for kinetic analysis. Figure 3.8 shows a linear relationship between the observed peak reduction current and the hydrogen peroxide concentration within the concentration range studied.

This correlation between the peroxide concentration and the peak reduction current corresponds to the enzyme kinetic case where the substrate concentration is lower than the apparent Michaelis-Menten constant, K'_M , and this Michaelis-Menten kinetic is given as:

$$I = I_{\max} [H_2O_2] / ([H_2O_2] + K'_M) \quad \text{Eq. 3.3}$$

where I is the observed catalytic current, I_{\max} is the maximum obtainable current for the biosensor, and $[H_2O_2]$ is the bulk solution concentration of hydrogen peroxide.



This can then be simplified to:

$$I = (I_{\max} / K'_M) [H_2O_2] \quad \text{Eq. 3.4}$$

The slope of the above plot, I_{\max}/K'_M represents the sensitivity of the biosensor and was found to be $2.88 \times 10^{-2} \text{ A mol}^{-1} \text{ dm}^3$. The reason for such a low sensitivity could be attributed to a low protein concentration used in the immobilisation process, (0.08 g l^{-1} for this study), the low D_e obtained (as compared to Iwuoha *et al.*) and the low purity of the enzyme used (type II HRP).

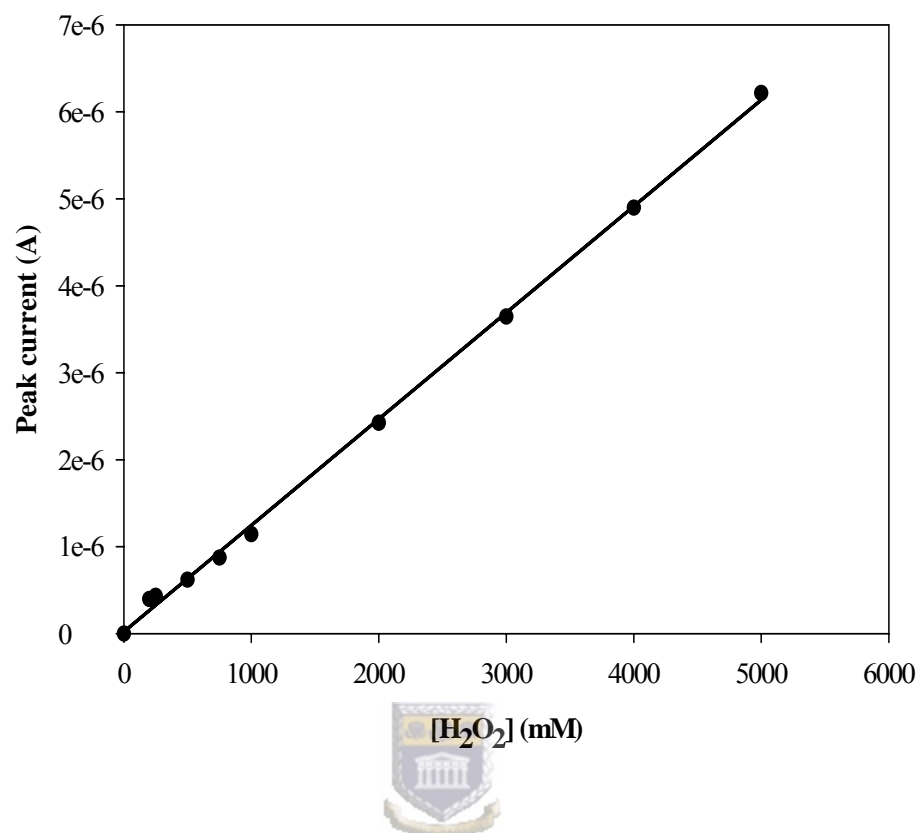


Figure 3.7.3: Calibration curve obtained with Pt/PANI/HRP biosensor for different [H₂O₂] against peak current. Experimental conditions are as in Figure 3.7.1.

Similar biosensor formats have been reported and it has been shown that optimum performance is achieved when much higher concentrations of HRP were used for immobilisation, specifically between 0.6 g l^{-1} and 0.75 g l^{-1} [44,88].

Below this concentration level, it was found that surface coverage was not maximised leading to low signals, while at concentrations higher than 0.75 g l^{-1} ; the response of the biosensor diminished, attributed to steric hinderance and hence, impeded electron transfer. However up to a concentration level of about 0.6 g l^{-1} , increases in sensitivity have been consistently reported [38,43].

The linear range for peroxide concentration was between 2.5×10^{-4} and 5.0×10^{-3} M and r^2 was 0.995.



3.2.2. Spectroelectrochemistry (SEC)

An optically transparent thin layer electrode (OTTLE) consisted of a piece of Pt mesh as a working electrode, contained in specially designed quartz cell containing the Ag/AgCl and Pt wire as a reference and auxiliary electrodes, respectively. The perforations in the platinum mesh were of such a size that the OTTLE transmitted sufficient visible light, whilst the electrode could still behave essentially as though it was planar. Polyaniline was immobilised on this Pt mesh according to Section 2.3.4 to fabricate a Pt/PANI electrode. This electrode was then used to monitor the reduction of hydrogen peroxide in the presence of HRP (0.08 g l^{-1}) in a bulk solution of phosphate buffer, pH 6.8.

The UV-Vis electronic spectrum of HRP only in the bulk solution, showed an absorption peak at approximately 400 nm [89,90] in the sorbet region, spectrum not shown, which is directly related to the active site microenvironment of the protein [91].

There was no noticeable difference between the spectra at zero potential, open circuit potential (OCP) and when the applied potential was -350 mV. This shows that the active site of the HRP enzyme was readily accessible in bulk solution at both potentials.

The addition of hydrogen peroxide to this solution resulted in the disappearance of the absorption band at 400 nm and the appearance of a new absorption band at 500 nm. This change in spectra can be attributed to the change in optical properties of the HRP on catalytic reduction of H_2O_2 . Once again, the catalytic reduction between HRP and H_2O_2 was not influenced by applied potential.

3.2.3. Scanning Electron Microscopy Analysis (SEM)

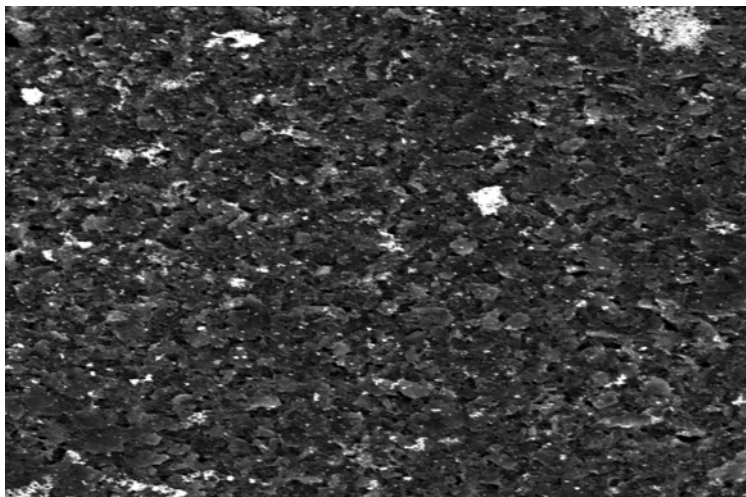
Scanning electron microscope studies were carried out on screen-printed carbon electrodes (SPCE) to study the topography of the electrodes. Figure **3.8.a** shows the surface of a typical SPCE. The surface topography showed good definition of graphite particles. The growth of PANI from an acidic medium, resulted in a sponge-like, branched, porous-structured, high-surface area polymer film on a SPCE, ideal for inclusion of enzyme, Figure **3.8.b**. The morphology of the PANI film is influenced by the nature of the electrolyte used [5,60].

The enzyme immobilisation can be observed by a change in topology to a speckled, grainy image as shown in Figure **3.8.c**, each of the speckles representing clusters of protein on the surface of the polymer [98].

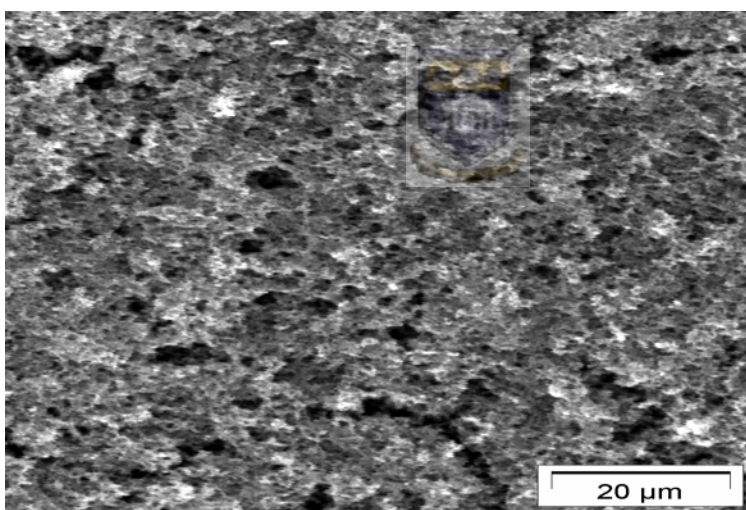


Following the performance of a cyclic voltammetry in the presence of 1 mM H_2O_2 , the morphology of the enzyme layer underwent a change, Figure **3.8.d**. The many clusters of protein observed in Figure **3.8.c** lessened, and the polymer layer beneath the protein could be seen clearly again. This deterioration in enzyme coverage may be due to the fact that a weak electrostatic immobilisation method was employed and leaching of the enzyme into the bulk solution upon application of potential occurred. Another reason may be due to HRP inhibition by high concentration of H_2O_2 .

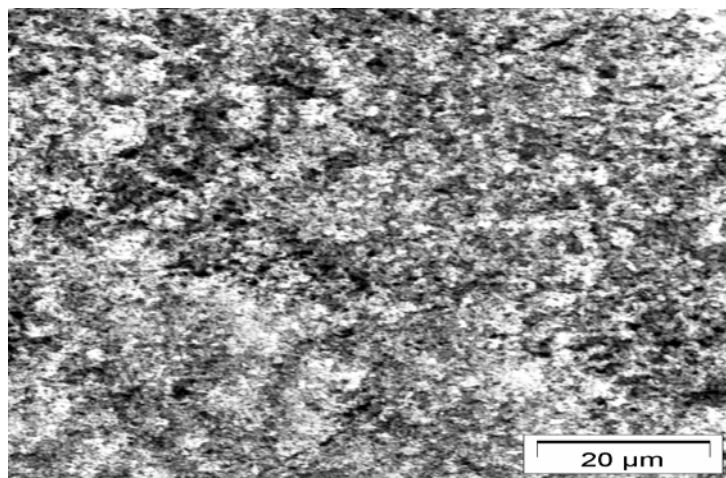
(a)



(b)



(c)



(d)

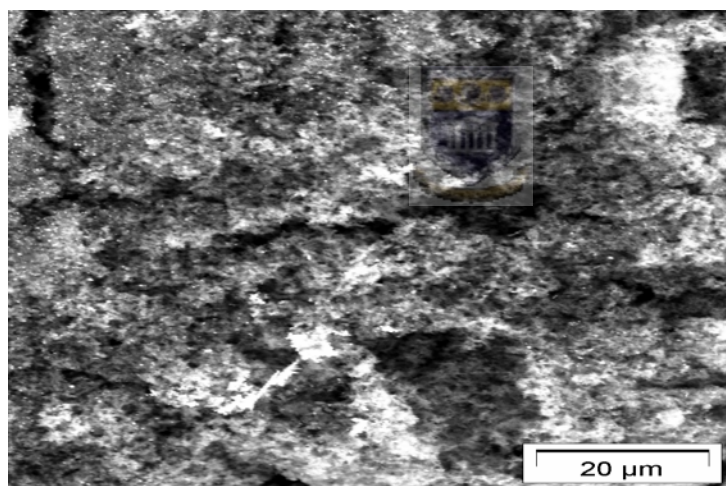


Figure 3.8: SEM images of screen-printed electrodes (area, 0.09 cm^2): (a) bare SPE, (b) PANI-modified, (c) PANI/HRP-modified, and (d) PANI/HRP (in the presence of $1 \text{ mM H}_2\text{O}_2$)-modified SPEs, respectively. The accelerating voltage and magnification for all the images were 15 kV and 1500x, respectively.

3.3. Cytochrome P450_{2D6}-Based Biosensor

The cytochrome P450-containing monooxygenase systems have long been the subject of active research owing to their essential role in the metabolism of a wide variety of compounds-both endogenous (steroids, fatty acids, hormones) and exogenous (drugs, toxins, carcinogens, mutagens) [92]. Although some electrochemical aspects of CYP450 have been reported [93], the direct, non-promoted electrochemistry of CYP450 is rather difficult to obtain with non-modified electrodes. The enzyme passivates the electrode and is denatured [94].

Serotonin reuptake inhibitors (SRIs) lack many of the adverse side effects of the older antidepressants, tricyclic antidepressants (TCAs) [78].

Achieving an electrical communication between an electrode and an enzyme is the pivotal step in the development of amperometric biosensors [3]. However, usually the protein matrix may insulate the redox site from direct electron transfer. While various enzyme immobilisation techniques have been reported to establish electrical communication in enzyme-electrode assemblies, with respect to CYP450 biosensors [27-28], there are currently only a few reports available. Most studies used the soluble cytochrome P450_{cam} (CYP101) enzyme [24-26,34-35].

3.3.1. CV Analysis of Fluoxetine Metabolism by GC/PANI/CYP2D6 Biosensor

Cyclic voltammetry was used to study the effect of fluoxetine on the electroactivity of the CYP2D6-based biosensor. Figure 3.9 shows the voltammetric responses of the PANI/CYP2D6-loaded glassy carbon electrode in the absence and presence of fluoxetine. Two distinct peaks, one anodic peak ($E_{p,a} = +540$ mV) and one cathodic peak ($E_{p,c} = -460$ mV) were observed in the absence of fluoxetine. The anodic peak potential and the corresponding peak current became less intense with addition of fluoxetine. The amperometric responses of the biosensor were measured at the cathodic peak potential of -460 mV against Ag/AgCl for different concentrations of fluoxetine in phosphate buffer solution.

Addition of fluoxetine to the oxygenated buffer solution caused a concentration-dependent increase in the reduction current in cyclic voltammetric experiments. Voltammograms showed a markedly increase in the reduction peak current upon addition of fluoxetine. At high concentrations of fluoxetine the biosensor response dropped. This suggests a case of substrate inhibition, which agrees with what has been observed by other workers on CYP2D6 [28,95-96]. This confirms that fluoxetine can act as both the substrate and inhibitor of CYP2D6 isoform. However, within experimental errors, the peak potential did not shift on addition of fluoxetine, thus the binding of fluoxetine as the substrate did not lower the redox potential of CYP2D6 as expected [27-28].

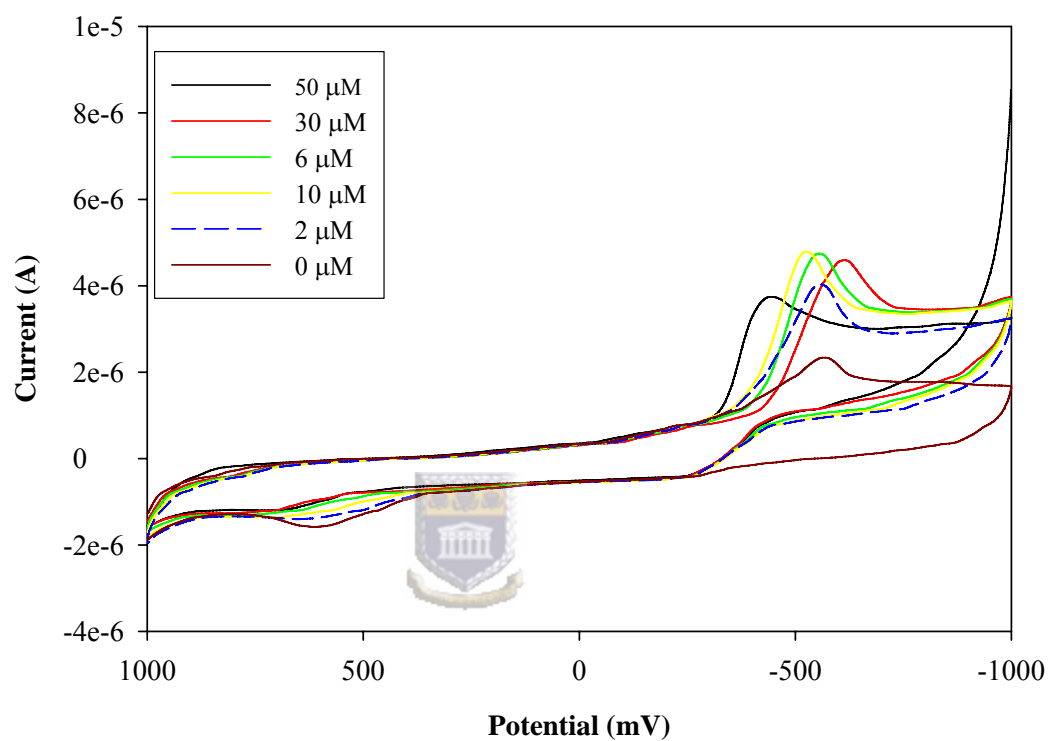


Figure 3.9: Cyclic voltammetric responses of GC/PANI/CYP2D6 biosensor to different concentrations of fluoxetine. Conditions: Oxygen-saturated phosphate buffer solution and a scan rate of 10 mV s^{-1} .

3.3.2. DPV Analysis of Fluoxetine Metabolism by CYP2D6 Biosensor

Differential pulse voltammetry was also carried out to study the reactivities of CYP2D6-based biosensor with fluoxetine. Figure 3.10.1 shows the response of the biosensor in the presence of different concentrations of fluoxetine. The DPV was performed in a reductive mode from an initial potential of 1000 mV to a final potential of -1000 mV. Other experimental conditions: scan rate of 20 mV s⁻¹, pulse amplitude of 50 mV, sample width, pulse width and pulse period was 17 ms, 50 ms and 200 ms, respectively.

Two DPV peaks were observed in the absence of fluoxetine as a substrate at +50 mV and -360 mV. It is also evident from the DP voltammograms that the current was dependent on fluoxetine concentration. The reductive current was monitored at the peak potential of +50 mV since the one at -360 mV was becoming less prominent with increase in fluoxetine. The DPV shows that the sensor can be used to monitor fluoxetine at low potentials where neither oxygen nor direct oxidation of its metabolites will interfere.

The same inhibition behaviour of fluoxetine at high concentration was also observed. The results from this study, like those obtained by other workers of CYP2D6 [95-96], have found the pharmacokinetics of the biotransformation of fluoxetine to be consistent with the non-competitive substrate inhibition model.

DP voltammograms were further analysed for kinetic parameters of CYP2D6. The calibration curve of GC/PANI/CYP2D6 biosensor at +50 mV, to different concentrations of fluoxetine was determined by DPV and is shown in Figure 3.10.2. The I_{\max} and Michaelis-Menten constant, K'_M , estimated from the plot of

peak current against [fluoxetine] were found to be 4.40×10^{-6} A and $3.786 \mu\text{M}$, respectively. This K'_M ($3.786 \mu\text{M}$), is comparable to what has been reported in the literature [28] and was found to be within the intra-hepatic fluoxetine concentration of between 2 and $7 \mu\text{M}$.

The plot of the linear range is shown in Figure **3.10.3**. The slope of the linear range corresponds to the sensitivity of the biosensor and corresponds to $1.247 \times 10^{-7} \text{ A } \mu\text{M}^{-1}$ ($r^2 = 99.8 \%$).



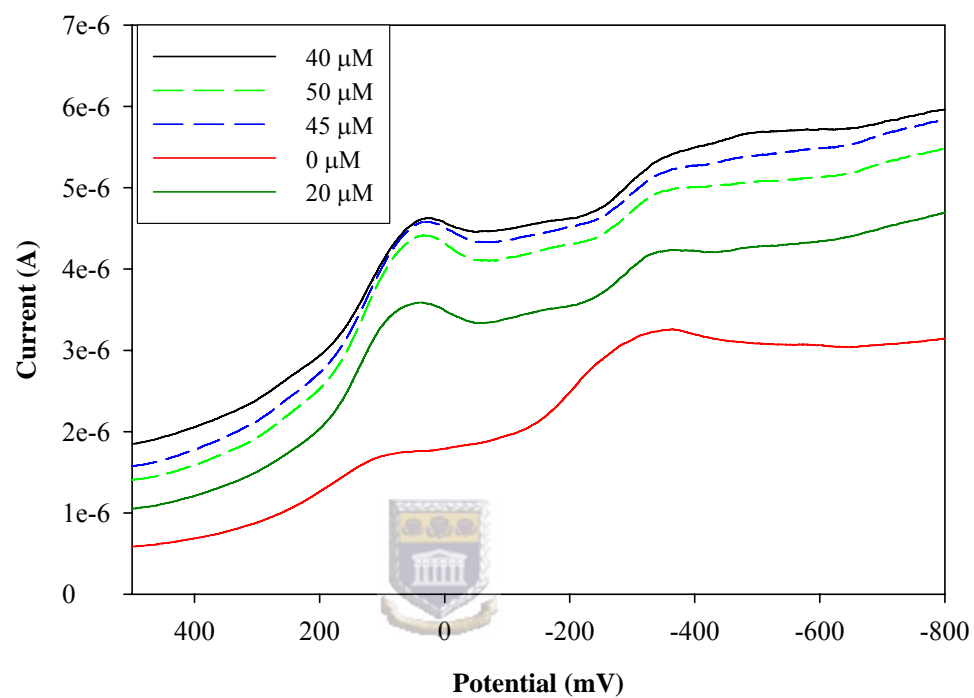


Figure 3.10.1: DPV responses of CYP2D6-based biosensor to fluoxetine. Experimental conditions buffer solution and scan rate 20 mV s^{-1} . The dotted lines show inhibition by fluoxetine.

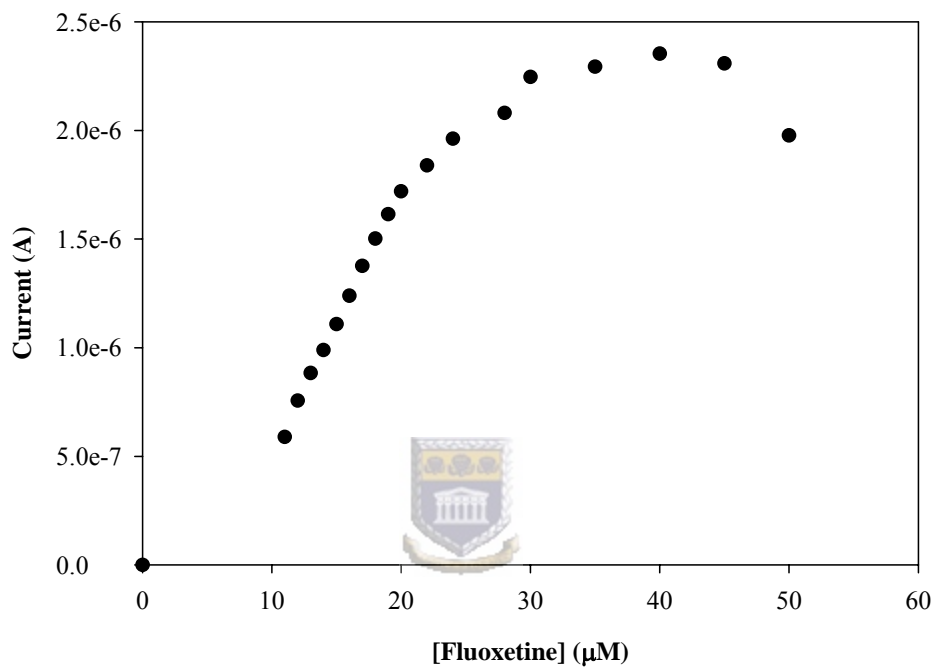


Figure 3.10.2: A plot of current against different concentrations of fluoxetine. The experimental conditions were: scan rate of 20 mVs^{-1} in an oxygen saturated buffer solution.

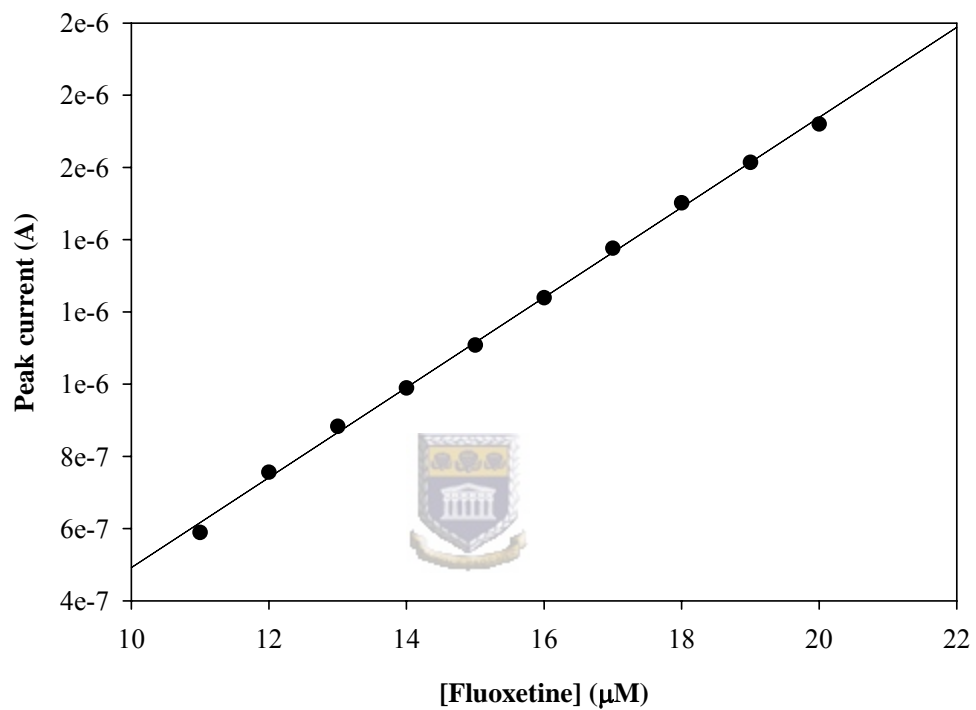


Figure 3.10.3: Linear range of CYP2D6 biosensor in the presence of fluoxetine in buffer solution. Experimental conditions are as in Fig. 3.10.1.

The serotonin reuptake inhibitor, fluoxetine is one of the mostly and extensively prescribed antidepressant throughout the world [96]. Fluoxetine is primarily metabolised in the liver to its active metabolite, norfluoxetine. This metabolite has the same pharmacological activity as the parent compound. Interindividual differences in fluoxetine metabolism are a major source for differences in the clinical response towards this drug [76].

The N-demethylation reaction of cytochrome P450_{2D6} (CYP2D6), under physiological conditions follows the monooxygenation pathway in which NADPH provides the two electrons that drive the reaction.

In the case of these amperometric biosensors, the electrons required for the monooxygenation reaction were provided by applying the appropriate potential through the GC/PANI/CYP2D6 electrode. The possible reaction scheme for the biosensor for N-demethylation of fluoxetine is summarised in Figure 3.11.

Under aerobic conditions, the second electron required in the monooxygenation reaction is used for the cleavage of di-oxygen, leading to the formation of several oxoferryl intermediates in the N-demethylation of fluoxetine to norfluoxetine [28].

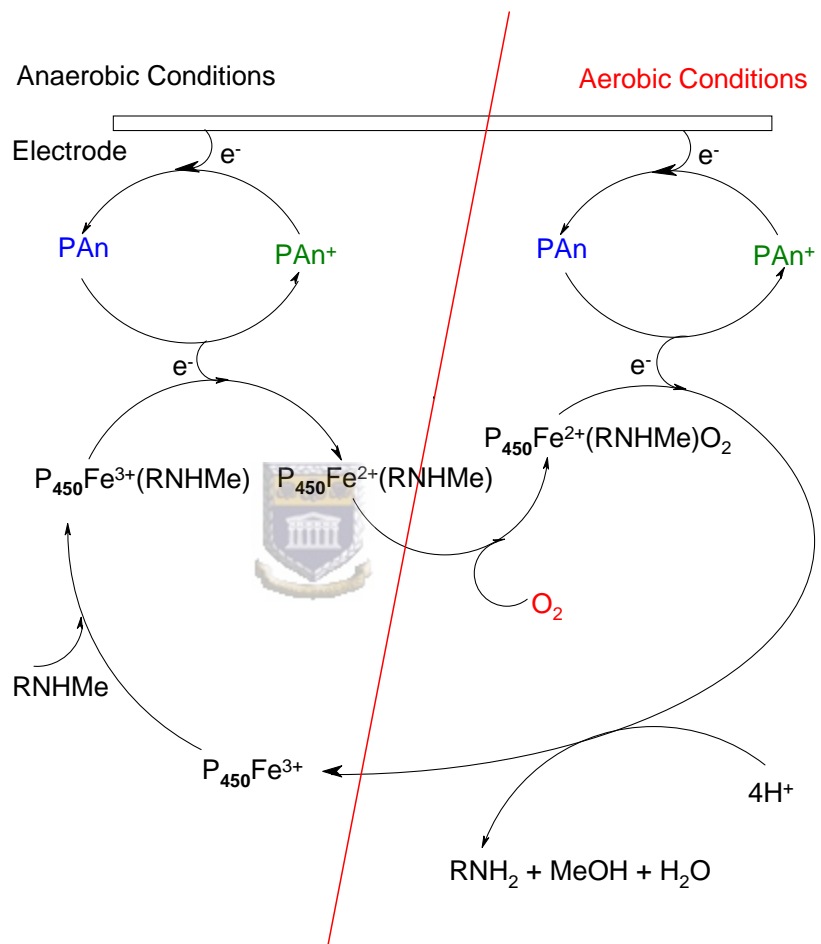


Figure 3.11: Catalysis reaction for CYP2D6 N-demethylation of fluoxetine at the polyaniline-modified electrode.

3.3.3. Other SRIs Analysis by GC/PANI/CYP2D6 Biosensor

Cyclic voltammetry, at a scan rate of 10 mV s^{-1} was also performed for the other two SRIs, fluvoxamine and citalopram. The potential was cycled between an initial potential of 1000 mV to a final potential of -1000 mV in an oxygen-saturated phosphate buffer solution. Figure 3.13 shows the cyclic voltammetric response of CYP2D6-based biosensor in the presence of different concentrations of fluvoxamine.

Two prominent peaks in the absence of fluvoxamine were observed: cathodic peak potential at -550 mV and an anodic peak potential at $+420 \text{ mV}$. The cyclic voltammograms show an increase in the peak current at -550 mV with an increase in concentration. This peak potential shifted to lower potential in the presence of fluvoxamine.



Cyclic voltammetry under the same conditions as for fluvoxamine was carried out for citalopram at 10 mV s^{-1} . There was a concentration-dependent increase in current with increase in citalopram concentration, CV not shown. Plot of peak current against concentration of citalopram did not follow the Michaelis-Menten kinetics.

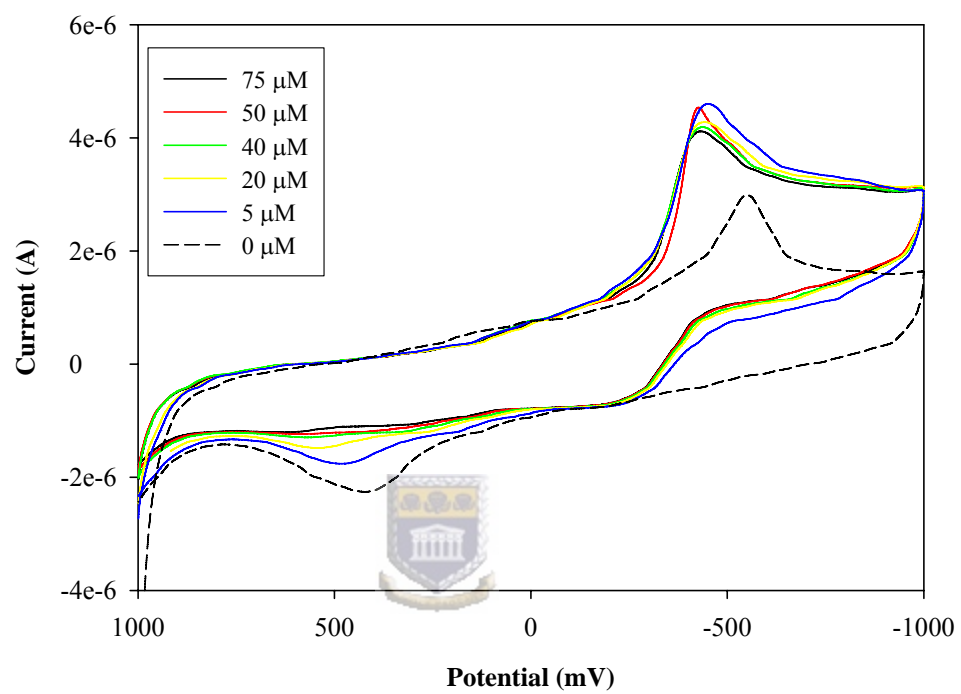


Figure 3.12: Voltammetric responses of CYP2D6 to fluvoxamine at a scan rate of 10 mV s^{-1} .

3.3.4. Analysis of Bufuralol using CYP2D6 Biosensor

The amperometric responses of the CYP2D6 biosensor for different concentrations of bufuralol were measured at the cathodic peak potential of -450 mV against Ag/AgCl. Figure 3.13.1 shows the CV responses of the CYP2D6-loaded glassy carbon electrode in the absence and in the presence of bufuralol. Cyclic voltammogram corresponding to 0 μM bufuralol has an anodic peak potential, $E_{p,a}$ of +540 mV and cathodic peak potential, $E_{p,c}$ of -450 mV. The anodic peak potential became less prominent with increase in concentration of bufuralol.

The voltammograms showed an increase in the reduction current upon the addition of bufuralol to the oxygen-saturated buffer solution. Plot of peak current against bufuralol concentration was consistent with Michaelis-Menten kinetics, Figure 3.13.2a. The maximum current, I_{max} and the apparent Michaelis-Menten constant, K'_M were 1.969 μA and 12.9 μM , respectively.

Figure 3.13.2b shows the linear range of the CYP2D6 biosensor has an upper limit of approximately 10 μM bufuralol ($r^2 = 99.9\%$). The slope of graph in Figure 3.13.2b corresponds to $1 \times 10^{-3} \mu\text{A } \mu\text{M}^{-1}$ and represents the sensitivity of the sensor.

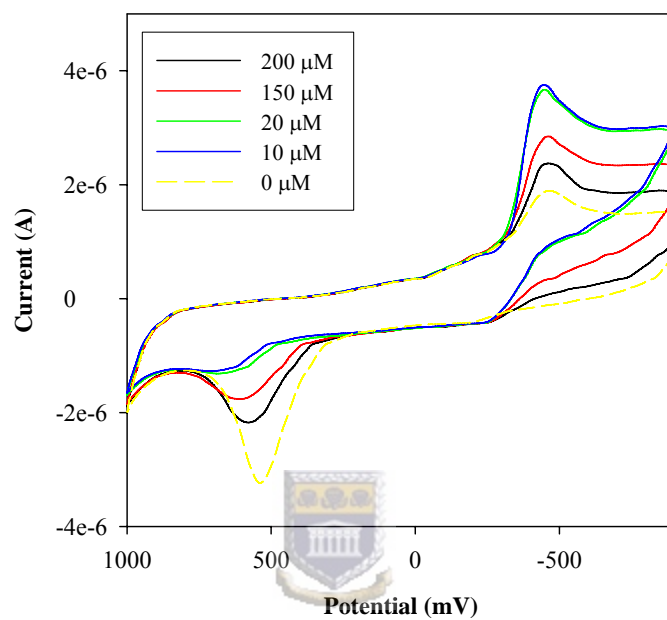


Figure 3.13.1: Voltammetric responses of GC/PANI/CYP2D6 biosensor to bufuralol. Experimental conditions were: oxygen-saturated phosphate buffer (pH 7.07, 0.1 M KCl) and scan rate of 10 mV s^{-1} . Dash line: 0 μM bufuralol, Solid lines: different concentrations of bufuralol.

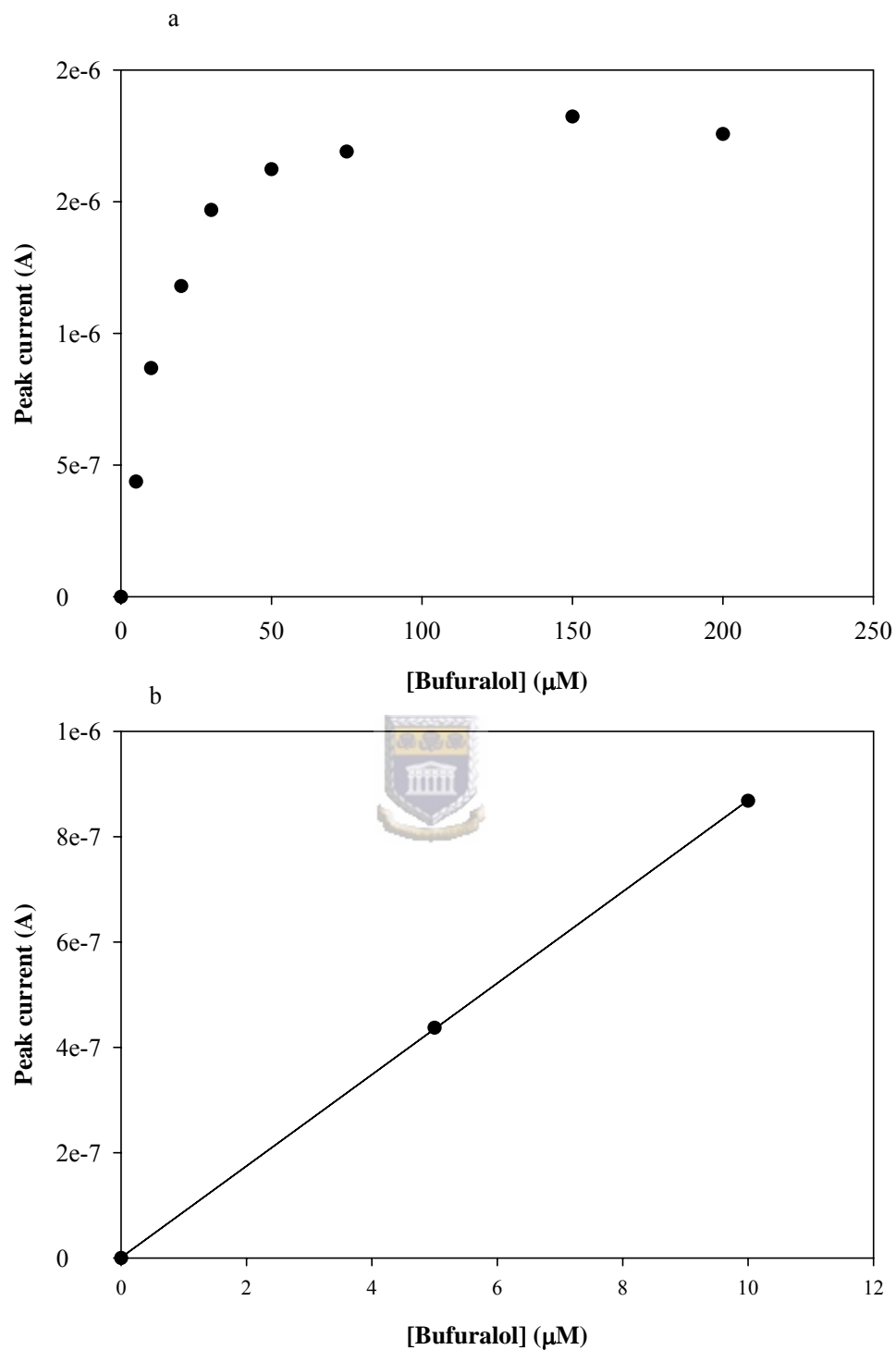


Figure 3.13.2: (a) Response curve of the CYP2D6-based biosensor to different concentrations of bufuralol at -450 mV. (b) Linear range calibration of CYP2D6 biosensor. Conditions are as in Fig. 3.13.1.

3.3.5. *Inhibition of CYP2D6 by Quinidine*

Cyclic voltammetry of quinidine in the presence of fluoxetine was performed at a scan rate of 10 mV s^{-1} . The potential was cycled from an initial potential of +1000 mV to a final potential of -1000 mV. Figure 3.14 shows the voltammetric response of CYP2D6 to fluoxetine in the presence of quinidine. It is clear from the voltammograms that the reductive current dropped in the presence of quinidine, confirming that quinidine inhibits the activity of CYP2D6.

The binding of quinidine slows the conversion of Fe^{3+} from low spin to high spin Fe^{3+} . Once Fe^{3+} has been converted to Fe^{2+} then the binding of oxygen becomes easy, O_2 binds easily to Fe in the 2+ oxidation state. By adding fluoxetine to the solution that already contains quinidine we are actually increasing the amount of oxygen in the system and the incubation of quinidine with CYP2D6. Since there's a 'fight' between fluoxetine and quinidine, this results in a decrease in peak current and a shift in reduction potential. Quinidine has been found to inhibit the activity of CYP2D6 even at lower concentrations.

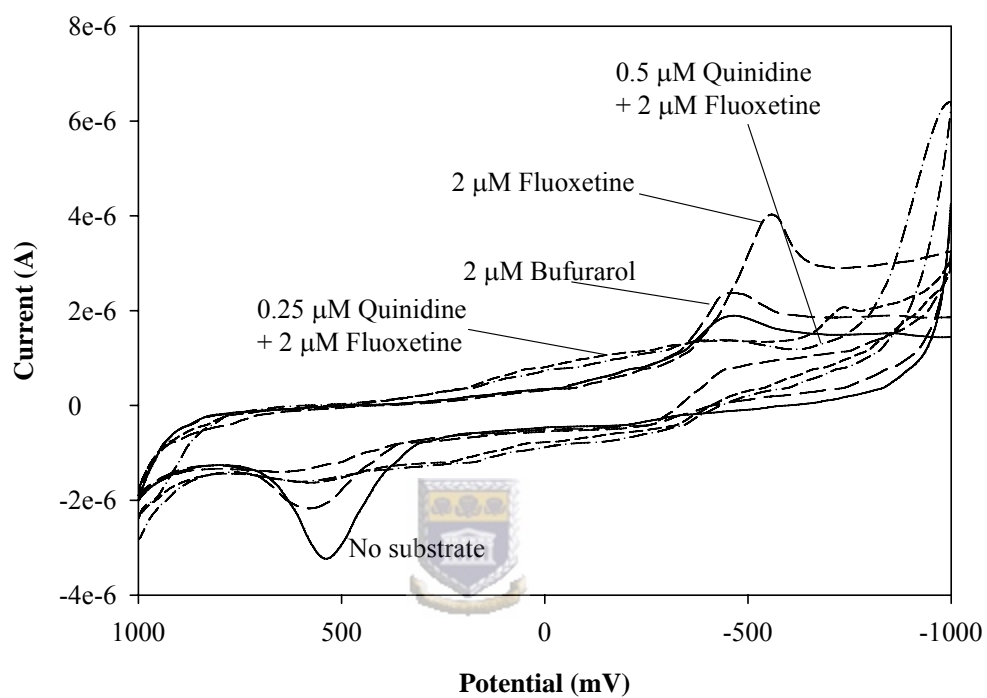


Figure 3.14: Voltammetric responses of GC/PANI/CYP2D6 biosensor to bufuralol, fluoxetine and quinidine. Scan rate 10 mV s^{-1} .

Table 3.1: Kinetic Parameters of CYP2D6 biosensors

Substrate	I_{\max} (μA)	K'_M (μM)	Sensitivity ($\mu\text{A} \cdot \mu\text{M}^{-1}$)
Fluoxetine	4.40	3.786	1.247×10^{-7}
Bufuralol	1.969	12.9	10^{-3}



CONCLUSIONS

The HRP based biosensor has been successfully prepared on the surface of Pt disk electrode using an immobilisation and mediation system based on the polymerisation of aniline. It is evident that the conducting polyaniline film not only acted as a matrix for immobilisation of HRP, but also as an electron-transferring medium during electrochemical process. The chemically modified electrode can catalyse the electroreduction of hydrogen peroxide between the concentration range of 1×10^{-5} and 4×10^{-3} M. Optimising the protein loading on the surface of the electrode could potentially increase the sensitivity of this biosensor. Although the analytical performance of the HRP-based biosensor is not as good as reported in the literature, this biosensor has several advantages such as control of the polymer film characteristics, good signal amplification, ease of fabrication and application to screen-printed electrodes for disposable use.

Electrochemical characterisation of the electroactive polymer, polyaniline, was carried out on the surface of glassy carbon electrode. This electroactive polymer was then successfully applied in the fabrication of CYP2D6-based biosensor. The PANI-modified biosensor was then used to observe the monooxygenation reaction of CYP2D6 with fluoxetine and other serotonin reuptake inhibitors (SRIs).

This study has found that modification of the glassy carbon electrode with a polyaniline film provided a suitable electrode surface for the bioelectrocatalytic

reaction between the heme centre of CYP2D6 enzyme in the presence of serotonin reuptake inhibitors (SRIs).

CYP2D6 has been well documented as exhibiting genetic polymorphism. As discussed in chapter 1, individuals are phenotyped according to the extent of drug metabolism they exhibit. The three phenotypes that have been put forward are: the poor metaboliser (PM), the extensive (normal) metaboliser (EM), and the ultra rapid metaboliser (URM). The percentages of the different types of metabolisers have been found to vary greatly within and across races. The genetic polymorphism exhibited by CYP2D6, and its role in determining drug clearance status in patients, have been documented by several research laboratories.

The combination of ease of preparation and control of the electrosynthesis of the film, allow this polyaniline-based bioelectrode to be a quick and reliable method for observing the reactivities of this monooxygenase enzyme in the monitoring of the antidepressant drugs, of the group serotonin reuptake inhibitors.

The study found that fluoxetine can act as both a substrate and an inhibitor for CYP2D6 isoenzyme. It has been concluded that in a scenario where CYP2D6 is the only enzyme responsible for the N-demethylation of fluoxetine, chronic use will result in accumulation of the drug but does not necessarily lead to CYP2D6 inhibition or denaturing.

The DPV shows that the sensor can be used to monitor fluoxetine at low potentials where neither oxygen nor direct oxidation of its metabolites will interfere.

REFERENCES

1. Clark, L. C. Jr., Lyons, C., 1962. Electrode systems for continuous monitoring in cardiovascular surgery. *Ann. NY Acad. Sci.*, 102: 29-45.
2. Turner, A. F. P., Karube, I., Wilson, G. S., (Eds.), 1987. *Biosensors: Fundamentals and Applications*, Oxford University Press, Oxford.
3. Wang, J., 1999. Amperometric biosensors for clinical and therapeutic drug monitoring: A review. *Journal of Pharm. and Biomed. Anal.*, 19: 47-53.
4. Cass, A. E. G., Davis, G., Francis, G. D., Hill, H. A. O., Aston, W. J., Higgins, I. J., Plotkin, E. V., Scott, L. D. L., Turner, A. P. F., 1984. Ferrocene-mediated enzyme electrode for amperometric determination of glucose. *Anal. Chem.*, 56: 667-671.
5. Cooper, J. C., Hall, E. A. H., 1992. Electrochemical response of an enzyme-loaded polyaniline film. *Biosensors & Bioelectronics*, 7: 473-485.
6. Wang, J., 2002. Review: Electrochemical nucleic acid biosensors. *Anal. Chim. Acta*, 469: 63-71.
7. Wang, J., Rivas, G., Cai, X., Palecek, E., Nielsen, P., Shiraishi, H. Dontha, N., Luo, D., Parrado, C., Chicharro, M., Farias, P. A. M., Valera, F. S., Grant, D. H., Ozsoz, M., Flair, M. N., 1997. DNA electrochemical biosensors for environmental monitoring: A review. *Anal. Chim. Acta*, 347: 1-8.
8. Lucarelli, F., Kicela, A., Palchetti, I., Marrazza, G., Mascini, M., 2002. Electrochemical DNA biosensor for analysis of wastewater samples. *Bioelectrochem.*, 58: 113-118.

9. Mariotti, E., Minunni, M., Mascini, M., 2002. Surface plasmon resonance biosensor for genetically modified organisms detection. *Anal. Chim. Acta*, 453: 165-172.
10. Evtugyn, G., Mingaleva, A., Budnikov, H., Stoikova, E., Vinter, V., Eremin, S., 2003. Affinity biosensors based on disposable screen-printed electrodes modified with DNA. *Anal. Chim. Acta*, 479: 125-134
11. Seki, A., Kawakubo, K., Iga, M., Nomura, S., 2003. Microbial assay for tryptophan using silicon-based transducer. *Sens. Actuat.*, 94: 253-256.
12. Rotariu, L., Bala, C., Magearu, V., 2004. New potentiometric microbial biosensor for ethanol determination in alcoholic beverages. (Article in Press)
13. Verma, N., Singh, M., 2003. A disposable microbial biosensor for quality control milk. *Biosens. Bioelectron.*, 18: 1219-1224.
14. Hock, B., 1997. Antibodies for immunosensors: A review. *Anal. Chim. Acta*, 347: 177-186.
15. Navrátilová, I., Skládal, P., Víklík, V., 2001. Development of piezoelectric immunosensors for measurement of albuminuria. *Talanta*, 55: 831-839.
16. Pemberton, R. M., Hart, J. P., Mottram, T. T., 2001. An electrochemical immunosensor for milk progesterone using a continuous flow system. *Biosens. Bioelectron.*, 16: 715-723.
17. Petrou, P. S., Kakabakos, S. E., Christofidis, I., Misiakos, K., 2002. Multi-analyte capillary immunosensor for the determination of hormones in human serum samples. *Biosens. Bioelectron.*, 17: 261-268.

18. Fatibello-Filho, O., Lupetti, K. O., Vieira, I. C., 2001. Chronamperometric determination of paracetamol using an avocado tissue (*Persea Americana*) biosensor. *Talanta*, 55: 685-692.
19. Abdelghani, A., Abdelghani-Jacquín, C., Hillebrandt, H., Sackmann, E., 2002. Cell-based biosensors for inflammatory agents detection. *Mat. Sci. Eng. C*, 22: 67-72.
20. Shinohara, H., Chiba, T., Aizawa, M., 1988. Enzyme microsensor for glucose with electrochemically synthesised enzyme-polyaniline film. *Sens. Actuat.*, 13: 79-86.
21. Iwuoha, E. I., Williams-Dottin, A. R., Hall, L. A., Morrin, A., Mathebe, G. N., Smyth, M. R., Killard, A., 2004. Electrochemistry and application of a novel monosubstituted squarate electron-transfer mediator in a glucose oxidase-doped poly(phenol) sensor. *Pure Appl. Chem.*, 76: 789-799.
22. Vijayakumar, A. R., Csöregi, E., Heller, A., Gorton, L., 1996. Alcohol biosensors based on coupled oxidase-peroxidase systems. *Anal. Chim. Acta*, 327:223-234.
23. Ivanov, A. N., Lukachova, L. V., Evtugyn, G. A., Karyakina, E. E., Kiseleva, S. G., Budnikov, H. C., Orlov, A. V., Karpacheva, G. P., Karyakin, A. A., 2002. Polyaniline-modified cholinesterase sensor for pesticide determination. *Bioelectrochem.*, 55: 75-77.
24. Iwuoha, E. I., Joseph, S., Zhang, Z., Smyth, M. R., Fuhr, U., Ortiz de Montellano, P. R., 1998. Drug metabolism biosensors: electrochemical reactivities of cytochrome P450_{cam} immobilised in synthetic vesicular systems. *J. Pharm. Biomed. Anal.*, 17: 1101-1110.

25. Iwuoha, E. I., Kane, S., Ania, C. O., Smyth, M. R., Ortiz de Montellano, P. R., Fuhr, U., 2000. Reactivities of organic phase biosensors: 3. Electrochemical study of cytochrome P450_{cam} immobilised in a methyltriethoxysilane sol-gel. *Electroanalysis*, 12:980-986.
26. Iwuoha, E. I., Smyth, M. R., 2003. Reactivities of organic phase biosensors: 6. Square-wave and differential pulse studies of genetically engineered cytochrome P450_{cam} (CYP101) bioelectrodes in selected solvents. *Biosens. Bioelectron.*, 18: 237-244.
27. Joseph, S., Rusling, J. F., Lvov, Y. M., Friedberg, T., Fuhr, U., 2003. An amperometric biosensor with human CYP3A4 as a novel drug screening tool. *Biochem. Pharmacol.*, 65: 1817–1826.
28. Iwuoha, E. I., Wilson, A., Howel, M., Mathebe, N. G. R., Montane-Jaime, K., Narinesingh, D., Guiseppi-Elie, A., 2004. Cytochrome P450_{2D6} (CYP2D6) bioelectrode for fluoxetine. *Anal. Lett.*, 37: 929-941.
29. Schubert, F., 1991. Mediated amperometric enzyme electrode incorporating peroxidase for the determination of hydrogen peroxide in organic solvents. *Anal. Chim. Acta*, 245: 133-138.
30. Mulchandani, A., Wang, C-L., Weetall, h. H., 1995. Amperometric detection of peroxides with poly(anilinomethylferrocene)-modified enzyme electrodes. *Anal. Chem.*, 67:94-100.
31. Yabuki, S., Mizutani, F., Hirata, Y., 2000. Hydrogen peroxide determination based on a glassy carbon electrode covered with polyion complex membrane containing peroxidase and mediator. *Sens. Actuat. B*, 65: 49-51.

32. Huang, R., Hu, N., 2001. Direct electrochemistry and electrocatalysis with horseradish peroxidase in Eastman AQ films. *Bioelectrochem.* 54: 75-81.
33. Razola, S. S., Ruiz, B. L., Diez, N. M., Mark Jr, H. B., Kauffmann, J-M., 2002. Hydrogen peroxide ssensitive amperometric biosensor based on horseradish peroxidase entrapped in a polypyrrole electrode. *Biosens. Bioelectron.*, 17: 921-928.
34. Ivanov, Y. D., Kanaeva, I. P., Gnedenko, O. V., Pozdnev, V. F., Shumyantseva, V. V., Samenkova, N. F., Kuznetsova, G. P., Tereza, A. M., Schmid, R. D., Archakov, A. I., 2001. Optical biosensor investigation of interactions of biomembrane and water-soluble cytochromes P450 and their redox partners with covalently immobilized phosphatidylethanolamine layers. *J. Mol. Recognit.*, 14: 185-196.
35. Hara, M., Yasuda, Y., Toyotama, H., Ohkawa, H., Nozawa, T., Miyake, J., 2002. A novel ISFET-type biosensor based on P450 monooxygenases. *Biosens. Bioelectron.*, 17: 173-179.
36. Gopel, W., Hesse, J., Zemel, J. N. (Eds), 1991. *Sensors: A comprehensive survey*. VCH, Weinheim.
37. Chaubey, A., Malhotra, B. D., 2002. Review: Mediated biosensors. *Biosens. Bioelectron.*, 17: 441-456.
38. Tatsuma, T., Gondaira, M., Watanabe, T., 1992. Peroxidase-incorporated polypyrrole membrane electrodes. *Anal. Chem.*, 64: 1183-1187.
39. Cosnier, S., 1999. Biomolecule immobilization on electrode surfaces by entrapment or attachment to electrochemically polymerized films. A review. *Biosens. Bioelectron.*, 14: 443-456.

40. Tatsuma, T., Watanabe, T., 1991. Oxidase/oxidase bilayer-modified electrodes as sensors for lactate, pyruvate, cholesterol and uric acid. *Anal. Chim. Acta*, 242: 85-89.
41. Garguilo, M. G., Huynh, N., Proctor, A., Michael, A. C., 1993. Amperometric sensors for peroxide, choline and acetylcholine based on electron transfer between horseradish peroxidase and a redox polymer. *Anal. Chem.*, 65: 523-528.
42. Iwuoha, E. I., de Villaverde, D. S., Garcia, N. P., Smyth, M. R., Pingarron, J. M., 1997. Reactivities of organic phase biosensors. 2. The amperometric behaviour of horseradish peroxidase modified with an electrosynthetic polyaniline film. *Biosens. Bioelectron.*, 12: 749-761.
43. Yang, Y., Mu, S., 1997. Bioelectrochemical responses of the polyaniline horseradish peroxidase. *J. Electroanal. Chem.*, 432:71-78.
44. Morrin, A., Guzman, A., Killard, A. J., Pingarron, J. M., Smyth M. R., 2003. Characterisation of horseradish peroxidase immobilised on an electrochemical biosensor by colorimetric and amperometric techniques. *Biosens. Bioelectron.*, 18: 715-720.
45. Gündoğan-Paul, M., Çelebi, S. S., Özyörük, H., Yildiz, A., 2002. Amperometric enzyme electrode for organic peroxides determination prepared from horseradish peroxidase immobilised in poly(vinylferrocenium). *Biosens. Bioelectron.*, 17: 875-881.
46. Sun, C., Li, W., Sun, Y., Zhang, X., Shen, J., 1999. Fabrication of multilayer films containing horseradish peroxidase based on electrostatic

interaction and their application as a hydrogen peroxide sensor. *Electrochim. Acta*, 44: 3401-3407.

47. Killard, A. J., Rocher, R., Mailley, P., O'Kennedy, R., Smyth, M. R., 1998. A screen-printed immunosensor based on polyaniline. Presented at INABIS '98-5th Internet World Congress on Biomedical Sciences at McMaster University, Canada, Dec 7-16th.
48. Bidan, G., Billon, M., Livache, T., Mathis, G., Roget, A., Torres-Rodriguez, L. M., 1999. Conducting polymers as a link between biomolecule and microelectronics. *Synth. Met.*, 102: 1363-1365.
49. Gerard, M., Chaubey, A., Malhotra, B. D., 2002. Review: Application of conducting polymers to biosensors. *Biosens. Bioelectron.*, 17: 345-359.
50. Brahim, S., Wilson, A. M., Narinesingh, D., Iwuoha, E. I., Guiseppi-Elie, A., 2003. Chemical and biological sensors based on electrochemical detection using conducting electroactive polymers. *Microchim. Acta*, 143: 123-137.
51. Mu, S., Chen, C., Wang, J., 1997. The kinetic behaviour for the electrochemical polymerization of aniline in aqueous solution. *Synth. Met.*, 88:249-254.
52. Bernard, M. C., Hugot-Le Goff, A., Joiret, S., Phong, P. V., 2001. Polyaniline films for protection against corrosion. *Synth. Met.*, 119:283-284.
53. Kraljić, M., Mandić, Z., Duić, Lj., 2003. Inhibition of steel corrosion by polyaniline coatings. *Corr. Sci.*, 45:181-198.

54. Mirmohseni, A., Solhjo, R., 2003. Preparation and characterisation of aqueous polyaniline battery using modified polyaniline electrode. *Eur. Pol. J.*, 39: 219-223.
55. Malta, M., Gonzalez, E. R., Torresi, R. M., 2002. Electrochemical and chromogenic relaxation processes in polyaniline films. *Pol.*, 43: 5895-5901.
56. Wang, J., 1991. Modified electrodes for electrochemical sensors. *Electroanalysis*, 3: 255-259.
57. Iwuoha, E. I., Smyth, M. R., 1996. Polymer-based amperometric biosensors, in: Lyons, M. E. G. (Ed.), *Electroactive Polymer Electrochemistry*, Plenum Press, New York, pp. 297-325.
58. Genies, E. M., Tsintavis, C., 1985. Redox mechanism and eletcrochemical behaviour of polyaniline deposits. *J Electroanal. Chem.*, 195: 109-128.
59. Schuhmann, W., Kranz, C., Wohlschläger, H., Strohmeier, J., 1997. Pulse technique for the electrochemical deposition of polymer films on electrode surfaces. *Biosens. Bioelectron.*, 12: 1157-1167.
60. Prasad, K. R., Munichandraiah, N., 2001. Potentiodynamic deposition of polyaniline on non-platinum metals and characterisation. *Synt. Met.*, 123: 459-468.
61. Sherman, B. C., Euler, W. B., Forcé, R. R., 1994. Polyaniline-A conducting polymer. *J. Chem. Educ.*, 71:A94-A96.
62. Csöregi, E., Gorton, L., Marko-Varga, G., 1994. Peroxidase-modified carbon fiber microelectrodes in flow-through detection of hydrogen peroxide and organic peroxides. *Anal. Chem.*, 66: 3604-3610.

63. Adeyoju, O., Iwuoha, E. I., Smyth, M. R., 1994. Amperometric determination of butanone peroxide and hydroxylamine via direct electron transfer at a horseradish peroxidase-modified platinum electrode. *Anal. Proc. Anal. Comm.*, 31: 177-179.
64. Wang, J., Lin, Y., Chen, L., 1993. Organic phase biosensors for monitoring phenol and hydrogen peroxide in pharmaceutical antibacterial products. *Analyst*, 118: 277-280.
65. Tatsuma, T., Ariyama, K., Oyama, N., 1996. Peroxidase-incorporated hydrophilic polythiophene electrode for the determination of hydrogen peroxide in acetonitrile. *Anal. Chim. Acta*, 318: 297-301.
66. Smit, M. H., Cass, A. E. G., 1990. Cyanide detection using a substrate-regenerating, peroxidase-based biosensor. *Anal. Chem.*, 62: 2429-2436.
67. Adeyoju, O., Iwuoha, E. I., Smyth, M. R., 1995. Reactivities of amperometric organic phase peroxidase-modified electrodes in the presence and absence of thiourea and ethylenethiourea as inhibitors. *Anal. Chim. Acta*, 305: 57-64.
68. Tatsuma, T., Oyama, N., 1996. H₂O₂-generating peroxidase electrodes as reagentless cyanide sensors. *Anal. Chem.*, 68: 1612-1615.
69. Ortiz de Montellano, P. R., 1995. Cytochrome P450 Structure, Mechanism and Biochemistry. 2nd edn., Plenum Press, New York.
70. http://www.preskorn.com/books/ssri_s7.html
71. Smith, D. A., Ackland, M. J., Jones, B. C., 1997. Properties of cytochrome P450 isoenzymes and their substrates. Part 2: properties of cytochrome P450 substrates. *DDT.*, 2: 479-487.

72. Honeychurch, M. J., Hill, H. A. O., Wong, L-L., 1999. The thermodynamics and kinetics of electron transfer in the cytochrome P450_{cam} enzyme system. FEBS Lett., 451: 351-353.
73. Reipa, V., Mayhew, M. P., Vilker, V. L., 1997. A direct electrode-driven P450 cycle for biocatalysis. Proc. Natl. Acad. Sci., USA. 94: 13554-13558.
74. Zhang, Z., Nassar, AE. F., Lu, Z., Schenkman, J. B., Rusling, J. F., 1997. Direct electron injection from electrodes to cytochrome P450_{cam} in biomembrane-like films. J. Chem. Soc., Far. Trans., 93: 1769-1774.
75. Shimada, T., Yamazaki, H., Mimura, M., Inui, Y., Guengerich, F. P., 1994. Inter-individual variations in human liver cytochrome P450 enzymes involved in the oxidation of drugs, carcinogens and toxic chemicals: studies with liver microsomes of 30 Japanese and 30 Caucasians. J. Pharmacol. Exp. Ther., 270: 414-423.
76. Bapiro, T. E., Hasler, J. A., Ridderstrom, M., Masimirembwa, C. M., 2002. The molecular and enzyme kinetic basis for the diminished activity of the cytochrome P450 2D6.17 (CYP2D6.17) variant. Potential implications for CYP2D6 phenotyping studies and the clinical use of CYP2D6 substrate drugs in some African populations. Biochem. Pharmacol., 64: 1387-1398.
77. [www.nzhp.org.nz/cytochrome P4502D6.pdf](http://www.nzhp.org.nz/cytochrome/P4502D6.pdf).
78. Rickels, K., Schweizer, E., 1990. Clinical overview of serotoninn reuptake inhibitors. J. Clin. Psychiatry, 51: 9-12.

79. Hemeryck, A., Belpaire, F. M., 2002. Selective serotonin reuptake inhibitors and cytochrome P450 mediated drug-drug interactions: an update. *Curr. Drug Metab.*, 3: 13-37.
80. Hiemke, C., Hartter, S., 2000. Pharmacokinetics of selective serotonin reuptake inhibitors. *Pharmacol. Ther.*, 85: 11-28.
81. van Harten, J., 1993. Clinical pharmacokinetics of selective serotonin reuptake inhibitors. *Clin. Pharmacokinet.*, 24: 203-220.
82. Christensen, M., Tybring, G., Mihara, K., Yasui-Furokori, N., Carrillo, J. A., Ramos, S. I., Anderson, K., Dahl, M-L., Bertilsson, L., 2002. Low daily 10-mg and 20-mg doses of fluvoxamine inhibit the metabolism of both caffeine and omeprazole (cytochrome P4502C19). *Clin. Pharmacol. Ther.*, 71: 141-153.
83. Rochat, B., Kosel, M., Boss, G., Testa, B., Gillet, M., Baumann, P., 1998. Stereoselective biotransformation of the selective serotonin reuptake inhibitor citalopram and its demethylated metabolites by mmonoamine oxidases in human liver. *Biochem. Pharmacol.*, 56: 15-23.
84. von Moltke, L. L., Greenbalt, D. J., Grassi, J. M., Granda, B. W., Venkatakrishnan, K., Duan, S. X., Fogelman, S. M., Harmatz, J. S., Shader,, R. I., 1999. Citalopram and desmethylecitalopram in vitro: Human cytochromes mediating transformation, and cytochrome inhibitory effects. *Biol. Psychiatry*, 46: 839-849.
85. Wedlund, P. J., de Leon, J., 2004. Cytochrome P450 2D6 and antidepressant toxicity and response: What is the evidence? *Clin. Pharmacol. Ther.*, 75: 373-375.

86. Bard, A. J., Faulkner, L. R., 2000. *Electrochemical Methods: Fundamentals and Applications*, 2nd Ed., Wiley, New York.
87. Mao, L., Yamamoto, K., 2000. Glucose and choline on-line biosensors based on electropolymerised Meldola's blue. *Talanta*, 51: 187-195.
88. Killard, A. J., Micheli, L., Grennan, K., Franek, M., Kolar, V., Moscone, D., Palchetti, I., Smyth, M. R., 2001. Amperometric separation-free immunosensor for real-time environmental monitoring. *Anal. Chim. Acta*, 427: 173-180.
89. Santucci, R., Laurenti, E., Sinibaldi, F., Ferrari, R. P., 2002. Effect of dimethyl sulfoxide on the structure and the functional properties of horseradish peroxidase as observed by spectroscopy and cyclic voltammetry. *Biochim. et Biophys. Acta*, 1596: 225-233.
90. Jones, D. K., Dalton, D. A., Rosell, F. I., Raven, E. L., 1998. Class I heme peroxidase: characterization of soybean ascorbate peroxidase. *Arch. Biochem. Biophys.*, 360: 173-178.
91. Ferri, T., Poscia, A., Santucci, R., 1998. Direct electrochemistry of membrane-entrapped horseradish peroxidase. Part I. A voltammetric and spectroscopic study. *Bioelectrochem. Bioenerg.*, 44: 177-181.
92. Sakaki, T., Inouye, K., 2000. Review: Practical application of mammalian cytochrome P450. *J. Biosci. Bioeng.*, 90: 583-590.
93. Kazlauskaitė, J., Westlake, A. C. G., Wong, L-L., Hill, H. A. O., 1996. Direct electrochemistry of cytochrome P450cam. *Chem. Comm.*, 2189-2190.

94. Lei, C., Wollenberger, U., Jung, C., Scheller, F. W., 2000. Clay-bridged electron transfer between cytochrome P450cam and electrode. *Biochem. Biophys. Res. Comm.*, 268: 740-744.
95. von Moltke, L. L., Greenbalt, D. J., Duan, S. X., Schmider, J., Wright, C. E., Harmatz, J. S., Shader, R. I., 1997. Human cytochromes mediating N-demethylation of fluoxetine in vitro. *Psychopharmacol.*, 132: 402-407.
96. Margolis, J. M., O'Donnell, J. P., Mankowski, D. C., Ekins, S., Obach, R. S., 2000. (R)-, (S)-, and racemic fluoxetine N-demethylation by cytochrome P450 enzymes. *Drug Met. Dispos.*, 28: 1187-1191.

